HHS Public Access

Author manuscript

Annu Rev Biophys. Author manuscript; available in PMC 2015 December 30.

Published in final edited form as:

Annu Rev Biophys. 2012 ; 41: 343–370. doi:10.1146/annurev-biophys-101211-113224.

Metabolite Recognition Principles and Molecular Mechanisms Underlying Riboswitch Function

Alexander Serganov[1] and **Dinshaw J. Patel**[2]

[1]Department of Biochemistry and Molecular Pharmacology, New York University School of Medicine, New York, New York 10016; alexander.serganov@nyumc.org [2]Structural Biology Program, Memorial Sloan-Kettering Cancer Center, New York, New York 10065; pateld@mskcc.org

Abstract

Riboswitches are mRNA elements capable of modulating gene expression in response to specific binding by cellular metabolites. Riboswitches exert their function through the interplay of alternative ligand-free and ligand-bound conformations of the metabolite-sensing domain, which in turn modulate the formation of adjacent gene expression controlling elements. X-ray crystallography and NMR spectroscopy have determined three-dimensional structures of virtually all the major riboswitch classes in the ligand-bound state and, for several riboswitches, in the ligand-free state. The resulting spatial topologies have demonstrated the wide diversity of riboswitch folds and revealed structural principles for specific recognition by cognate metabolites. The available three-dimensional information, supplemented by structure-guided biophysical and biochemical experimentation, has led to an improved understanding of how riboswitches fold, what RNA conformations are required for ligand recognition, and how ligand binding can be transduced into gene expression modulation. These studies have greatly facilitated the dissection of molecular mechanisms underlying riboswitch action and should in turn guide the anticipated development of tools for manipulating gene regulatory circuits.

Keywords

X-ray crystallography; ligand-binding pockets; NMR; RNA structure and folding; metal ions

INTRODUCTION

The major impact of RNA molecules on gene expression control has been highlighted by recent progress in riboswitch structure-function studies. Riboswitches are structured mRNA regions that directly sense cellular metabolites and respond to metabolite binding by modulating gene expression (85, 100, 131). Discovered about a decade ago (73, 80, 130), riboswitches constitute one of the major regulatory mechanisms that rival protein-based

DISCLOSURE STATEMENT

The authors are not aware of any affiliations, memberships, funding, or financial holdings that might be perceived as affecting the objectivity of this review.

genetic circuits in bacteria, with representatives found in archaea, plants, and fungi (111). The fortunate initial findings of several riboswitches in genetic systems that lacked metabolite-sensing regulatory proteins have subsequently developed into a pipeline that currently includes sophisticated genome-wide computer searches of sensing domains, cognate metabolite identification, and demonstration of metabolite-specific riboswitch action. To date, riboswitches comprise about 20 classes that respond to purines and their derivatives, amino acids, protein coenzymes, and a phosphorylated amino sugar (95). In addition to riboswitches that sense small organic molecules, RNAs can also utilize inorganic molecules, such as Mg^{2+} cations and fluoride anions, to trigger a regulatory response (6, 17, 19). The vast majority of riboswitches are located in the 5′ untranslated regions (UTRs) of mRNAs, although eukaryotic riboswitches also reside in introns situated within all regions of pre-mRNAs, including the central part and the 3′ UTR (8). The location of riboswitches within their mRNAs defines the regulatory targets of riboswitches. Practically all riboswitches modulate expression of genes encoded within the same mRNA molecules. Therefore, both the sensing and regulatory aspects of riboswitch function are spatially contained and represent an attractive model for biophysical elucidation, with the goal of understanding riboswitch mechanisms at the molecular level.

MECHANISMS OF RIBOSWITCH-MEDIATED CONTROL

Most riboswitches consist of two domains: an evolutionarily conserved sensing or aptamer module that recognizes cellular metabolite(s) and a nonconserved expression platform that contains signal(s) for gene expression control (85, 131). The genetic control is usually exerted through the metabolite-dependent formation of two mutually exclusive riboswitch conformations, which affect the availability of signals for the gene expression machinery. In the most typical riboswitch-mediated type of control, transcription attenuation, a cognate metabolite binds the sensing domain and stabilizes its metabolite-bound conformation. Stabilization of the sensing domain facilitates the formation of a downstream hairpin followed by a polyuridine tract that serves as a transcription terminator to prevent transcriptional elongation and gene expression (Figure 1). If the metabolite concentration is not sufficient to trigger the riboswitch response, the sensing domain does not adopt a stable metabolite-bound conformation and instead participates in the formation of an alternative antiterminator hairpin that allows for transcription elongation to proceed through the expression platform and the gene coding sequence, thereby turning gene expression on. The folding of alternative riboswitch conformations is based on the ability of the switching sequence (Figure 1) to be engaged in two different pairing alignments, either with a region of the sensor, thus forming domain-closing helix P1, or with a complementary sequence within the expression platform, thereby forming an antiterminator and preventing the formation of a transcription terminator.

Conserved sensing modules can be combined with a variety of expression platforms. In some riboswitches, transcriptional control is replaced by regulation at the level of translation (130), which is based on the accessibility of the ribosome-binding site (RBS) and initiation codon for ribosome entry. The ribosome cannot initiate translation if these elements are occluded, for instance, by the formation of a hairpin that contains base-paired RBSs. Although most riboswitches contain distinctive expression platforms and rely on the

interplay between regulatory helix P1 and alternative helix formation, some riboswitches deviate from this rule. The *S*-adenosylmethionine class III (SAM-III) riboswitch (28) does not possess a well-defined long expression platform and has its RBS sequestered within the metabolite-bound fold upon ligand binding. Regulation by SAM-II (30), adocobalamin (AdoCbl) (79), and prequenosine$_1$ (preQ$_1$) (45, 49, 108) riboswitches depends on the formation of a pseudoknot between the sensing domain and an outside sequence. Similarly, switching sequences or peripheral elements of the sensing domains from eukaryotic thiamine pyrophosphate (TPP) riboswitches can pair with splicing site sequences located outside sensing modules and provide the TPP-induced release of alternative splicing sites, which result in gene repression through premature translation termination in algae, short peptide translation in fungi, and production of unstable mRNA species in higher plants (121).

A conformational transition within riboswitches is not a prerequisite of riboswitch-dependent gene modulation. The *glmS* riboswitch/ribozyme does not switch its conformation at all (50, 133) and, upon glucosamine-6-phosphate (GlcN6P) binding, undergoes ligand-induced-specific self-cleavage, leading to the degradation of the downstream transcript by ribonuclease (RNase) J1 (14).mRNA degradation may also contribute to gene repression by other riboswitches. The Mg^{2+} riboswitch has been implicated in regulating susceptibility of the *mgtA* transcript to degradation by RNase E, a functional homolog to RNase J1, when bacteria are grown in high-Mg^{2+} environments (107). Message degradation could also be involved in the modulation of virulence factor PrfA in *Listeria monocytogenes* by the SAM SreA riboswitch, which, unlike the remainder of known riboswitches, can function in *trans* and act as a noncoding RNA (64).

The majority of riboswitch metabolites control gene products that are directly related to the biosynthesis, degradation, or transport of these metabolites. Depending on gene function, riboswitches can provide negative or positive feedback, the latter being less common (67).However, the recent finding of riboswitches that respond to bacterial second messenger cyclic di-guanosine monophosphate (c-di-GMP) suggests that riboswitches can trigger much wider-ranging physiological changes, including cell differentiation, conversion between motile and biofilm lifestyles, and virulence gene expression, and that they can be located within unexpected gene controlling systems, for instance, in the lysis module of the bacteriophage genome (113).

Riboswitches do not always function in isolation. Many genetic systems involve tandem arrangements of complete riboswitches that provide enhanced digital gene control in the case of the same riboswitch type or that serve as logic gates relaying independent signals in the case of riboswitches with distinct specificities (112). Representatives of glycine-specific riboswitches have two consecutive sensing domains capable of cooperative ligand recognition (68), with docking of the ligand at one site influencing the glycine binding to the second site. The regulatory effect of these paired motifs is exerted via a single expression platform and is maximized over a narrower range of glycine concentration. In addition, riboswitches can collaborate with other genetic elements to create even more complex controlling systems. The *Clostridium difficile* c-di-GMP riboswitch allosterically regulates the GTP-dependent self-splicing of group I ribozymes (57). This conjoined riboswitch-

ribozyme system unmasks the translation initiation codon and creates a perfect RBS for the translation of a putative virulence gene. In *Salmonella enterica*, the Mg^{2+} riboswitch apparently coordinates its action with the translation of a peptide encoded within the riboswitch sequence (87, 136). These findings illustrate the variety of regulatory strategies employed by cells to affect gene expression in response to cellular metabolites.

DIVERSITY OF RIBOSWITCH STRUCTURES

Despite the extensive diversity of expression platforms and regulatory mechanisms exploited by riboswitches, their ability to respond to selected compounds is entirely programmed in their conserved metabolite-sensing domains. The broad distribution of riboswitch ligands has been matched by the large variability of identified metabolite-sensing domains, which have been a subject of intensive structural studies. Within the last seven years, structural biologists have reported the high-resolution crystal and solution three-dimensional structures of 17 riboswitch classes, which overall represent most major riboswitch types with identified metabolite effectors. The availability of these primarily ligand-bound structures allows for direct comparison of representatives within riboswitch types as well as between distinct riboswitch families.

Purine-Related Riboswitches

Riboswitches triggered by purine bases, nucleosides, and nucleotides constitute an expansive and diverse group of purine-related sensors. This group combines riboswitches responsive to guanine (66), adenine (67), and 2′-deoxyguanosine (dG) (47), as well as two classes that are specific for the modified guanine base $preQ_1$ (72, 97). In addition, two classes selective for cyclic purine dinucleotide c-di-GMP (57, 113) can be grouped together with purine riboswitches on the basis of the chemical similarity of their ligands. The sensing domains of purine riboswitches range from 34 nucleotides (nt), currently the minimal size for a metabolite sensor, to ~90 nt, close to the average size of many metabolite-sensing domains. Structures determined for all purine riboswitches have revealed a three-way junction or a junction-like architecture for all RNAs, except the $preQ_1$ class I ($preQ_1$-I) riboswitch, which adopts a pseudoknot fold. Characteristic features of junctional purine riboswitches include the junctional positioning of the bound ligands and the presence of long-distance tertiary interactions that stabilize the overall riboswitch folds.

Virtually identical structures of adenine and guanine riboswitches bound to their cognate ligands adenine (102), guanine (102), and hypoxanthine (7) were the first reported crystal structures of ligand-bound riboswitches (Figure 2*a*,*b*). These structures are reminiscent of a tuning fork architecture, in which regulatory helix P1 forms the handle, and hairpins P2/L2 and P3/L3, connected through pairing at the top, represent the prongs. The ligand is buried inside the junctional core, where it is sandwiched between layers of nucleotide triplets and is surrounded by pyrimidine residues. The specificity of adenine and guanine riboswitches is defined primarily by Watson-Crick base-pairing to a single specificity-determining nucleotide at position 74, which is either uridine or cytosine, respectively (7, 66,67, 84, 102) (Figure 2*a*,*b*). Other core nucleotides demonstrate sequence restrictions (60, 77) that are required to prevent interactions of the junctional nucleotides with the discriminatory nucleotide (21), which can effectively replace ligand-riboswitch contacts and impair

riboswitch control (119). Structural and biochemical studies suggest that purine binding organizes the junction and facilitates the formation and stabilization of the regulatory helix P1 through stacking interactions and triple base-pairing with a flexible segment adjacent to the ligand-binding pocket.

The dG riboswitch features a global architecture similar to the fold of adenine and guanine riboswitches (88) (Figure 2*c*). Nevertheless, the dG riboswitch possesses several important changes in sequence within the ligand-binding pocket and peripheral regions. To prevent a clash with the sugar ring of dG, U51 is replaced by C58, which slides along the minor groove edge of the bound dG and forms alternative base-pairing with the ligand (23, 88) (Figure 2*c*). Additional changes in the A54-to-C57 segment ensure sufficient room and specific bonding to the dG sugar moiety. However, mutations in the core of the guanine riboswitch need to be supplemented by the introduction of original helix P2 and tertiary loops in order to convert the guanine riboswitch to the wild-type dG riboswitch (23). A likely explanation for this observation has come from the determination of the structure of the natural dG riboswitch, which shows that G33, located above the ligand-binding pocket, participates in the formation of a base triple in the P2 stem (88), whereas the corresponding A24 stays unpaired in the P3 stem of adenine and guanine riboswitches (Figure 2*c*). The new position of this purine residue might reinforce the stem regions to stabilize abbreviated tertiary loop base-pairing, which replaces extensive nucleotide quartet interactions of adenine/guanine riboswitches and features a key-and-lock insertion of A71 into the L3 loop in the dG riboswitch (Figure 2*c*).

The two structures of c-di-GMP riboswitches (54, 104, 105) emphasize the differences between RNAs that evolved to recognize the same ligand, albeit with different affinities. The riboswitches adopt distinct junctional folds (Figure 2*d*,*e*). The c-di-GMP-I riboswitch folds into a Y-shaped three-way junctional structure, with two long helices joined at the top by tetraloop-tetraloop receptor interactions (Figure 2*d*). In the c-di-GMP-II riboswitch, the long stem P2/P3/P4 reverses its orientation via a kink-turn motif and forms a tertiary pseudoknot with junctional nucleotides, creating a pseudo three-way junction, where the P4 helix is built by tertiary base-pairing (Figure 2*e*). Critical differences are also observed in the ligand-binding pockets. Despite similar stacking interactions that involve guanine bases of the ligand, adjacent RNA base pairs, and an adenine residue (A47 and A70) intercalated between guanine bases, the two ligands are recognized using different principles (Figure 2*d*,*e*). The guanine bases in the c-di-GMP-I riboswitch form extensive interactions using Watson-Crick (C92) and Hoogsteen edges (Figure 2*d*), whereas noncanonical interactions (involving A69 and G73) are formed between the ligand and the c-di-GMP-II riboswitch (Figure 2*e*). In addition, the phosphodiester backbone is extensively contacted in the c-di-GMP-I riboswitch but not in the c-di-GMP-II riboswitch, contributing to the higher affinity of class I for the ligand (103). As in the adenine, guanine, and dG riboswitches, the regulatory response depends on the ligand-induced stabilization of the junction that brings together 5′ and 3′ segments of the regulatory helix P1.

The class-I $preQ_1$ riboswitch adopts a compact H-type pseudoknot fold (45, 49, 108) (Figure 2*f*) that differs dramatically from the junctional architectures of other purine riboswitches (Figure 2*a*–*e*). The $preQ_1$ ligand is buried in the pseudoknot core, where it intercalates

between helical stacks and forms multiple hydrogen bonds using all available heteroatoms (Figure 2*f*). As in adenine/guanine riboswitches, the Watson-Crick edge of the ligand is recognized by canonical base-pairing with a cytosine (C19). The Watson-Crick base-pairing is unlikely to account for ligand recognition in the class-II $preQ_1$ riboswitch, although a pseudoknot is predicted to constitute the essential part of this riboswitch structure (72). In contrast to the junctional purine riboswitches, $preQ_1$ riboswitches exert their regulatory response by pairing with a downstream sequence, thereby preventing the formation of the antiterminator hairpin.

Amino Acid Riboswitches

In bacteria, amino-acid-related genes are typically controlled via a T-box system that involves interactions between corresponding uncharged tRNA molecules and mRNA regulatory regions (33). Nonetheless, three amino acids, glycine (68), lysine (34, 94, 114), and glutamine (3), target gene expression by interacting with their own riboswitches. Structural information is available for glycine (12, 40) and lysine (29, 98) riboswitches. The glycine riboswitch structure was determined in two forms: at moderate resolution for the cooperative *Fusobacterium nucleatum* glycine riboswitch (12), which comprises two similar sensing domains in a tandem arrangement, and at higher resolution for the isolated domain II (Figure 3*a*) of the *Vibrio cholerae* riboswitch (40).

Despite recognizing ligands of the same class, glycine and lysine sensors are remarkably dissimilar. The glycine riboswitch fold is based on a three-way junctional architecture stabilized by tertiary interactions between the junctional region and the adjoining glycine-binding pocket, which is embedded into the bottom part of the helical stem P3/P3a (Figure 3*a*). One of the largest metabolite-sensing domains, the lysine sensor adopts a much more complex fold that consists of two-helix and three-helix bundles radiating from a ligand-bound five-way junction (Figure 3*b*) and is stabilized by tertiary kissing-loop interactions between stem-loops P2/L2 and P3/L3. A notable feature of the lysine riboswitch is a reversion of the P2/L2 hairpin, reminiscent of the c-di-GMP-II riboswitch, facilitated through turns associated with loop E (16) and kink-turn (51) motifs (Figure 3*b*).

The two riboswitches also utilize distinct structural principles for ligand recognition. Glycine, together with two divalent cations (Mg1 and Mg2), is positioned within the widened helical structure outside the junction and is specifically recognized by conserved U69 and purine bases (Figure 3*a*). By contrast, lysine is encapsulated in a tight pocket between helices P2 and P4 in the heart of the junction (Figure 3*b*) and makes specific hydrogen bonds with the sugar edges of conserved purines (G12 and G114) and the backbone of other nucleotides. The distinct location of the binding pockets defines different mechanisms for regulatory helix P1 stabilization. The glycine riboswitch extrudes conserved adenine (A33) from the ligand-binding pocket (Figure 3*a*) and intercalates it into the junction, thus stabilizing the junctional region and adjacent helix P1. On the other hand, in the lysine riboswitch, the bound ligand stacks directly on the top pair of the P1 helix (Figure 3*b*) and organizes nucleotides around the upper portion of the helix, thereby contributing to its stability.

Regardless of the many differences, glycine and lysine recognition exhibits one striking similarity. The negative charge of the carboxylate moieties of both ligands is neutralized by interactions with metal cations, either Mg^{2+} (Mg2, Figure 3*a*) or K^{+} (Figure 3*b*) for glycine and lysine, respectively. Notably, the glutamine riboswitch, for which there is yet no structural information, is predicted to adopt a pseudoknot-based fold (3), most dissimilar to glycine and lysine riboswitches.

The unique feature of the tandem glycine riboswitch—cooperative glycine binding—was inferred to be dependent on tertiary interdomain interactions by biochemical experiments (55). Three pairs of tertiary interdomain contacts have been proposed on the basis of crystal-packing interactions in the crystals of the *Vibrio cholerae* domain II structure, nuclease footprinting experiments (40), and nucleotide analog interference mapping (55). Similar contacts in the structure of the tandem *F. nucleatum* glycine riboswitch were recently identified (12) (Figure 3*c*). These contacts, designated α−α′ and β−β′, are formed between nonpaired adenine-rich segments from loop L3 and junctional region J3a/3b that are inserted into the minor groove of helices P1 (Figure 3*d*). Additional interactions, designated γ−γ′, involve a noncanonical A·U base pair. Although the mechanism of the cooperative response is not understood, structural studies imply that the conformation of the contacting regions depends on glycine binding. Therefore, glycine binding to one domain could induce the formation of tertiary interactions that preorganize another domain and facilitate its ligand binding (40). This view is consistent with large conformational rearrangements observed upon glycine binding in solution by small-angle X-ray scattering (SAXS) experiments (63).

Coenzyme-Related Riboswitches

Riboswitches responsive to protein coenzymes, cofactors, and related compounds represent the most abundant and diverse group. This group includes AdoCbl (80), TPP (73, 130), molybdenum cofactor (Moco) (91), tungsten cofactor (Tuco) (91), flavin mononucleotide (FMN) (73, 132), tetrahydrofolate (THF) (4), and five classes of SAM (15, 27,28, 70, 89, 123, 125, 126, 134) riboswitches, as well as a riboswitch activated by *S*-adenosylhomocysteine (SAH) (123), a by-product of SAM-dependent methyl group transfer reaction. Three-dimensional crystal structures have been determined for the majority of coenzyme-specific riboswitches, except for AdoCbl, Moco/Tuco, SAM-IV, and SAM-V sensors (Figure 4). Although most coenzymes represent elongated molecules carrying aromatic ring systems toward one end and phosphate or amino acid moieties toward the other end, the RNA scaffolds that bind these compounds demonstrate striking architectural differences.

The fact that the structures do not look alike is especially intriguing, given that three of these riboswitches recognize SAM and one binds to chemically similar SAH. The SAM-I structure is based on a four-way junction fold reinforced by a pseudoknot and tertiary interactions between two helices, P1 and P3, which create a pocket for the ligand (74) (Figure 4*a*). The SAM-II riboswitch adopts an H-type pseudoknot conformation that comprises a continuous helix P1/P2b/P2a interacting with loops L1 and L3, with the bound SAM positioned along P2b (30) (Figure 4*b*). The structures of SAM-III (65) and SAH (24) riboswitches exhibit a remote visual similarity, because both riboswitches converge to

compact architectures with junctional positioning of the bound ligands (Figure 4*c*,*d*). Nevertheless, the SAM-III structure is based on a three-way junction topology, whereas the SAH riboswitch forms a rare LL-type pseudoknot.

In parallel with their overall architectures, the SAM/SAH riboswitches form drastically different ligand-binding pockets that interact with ligands adopting distinct conformations. Thus, in the SAM-I structure (74) (Figure 4*a*), SAM adopts a compact U-shaped conformation stabilized by intramolecular interactions involving stacked methionine and adenine moieties. This bound ligand conformation is specifically recognized by extensive hydrogen-bonding and electrostatic interactions to two distinct faces located in the minor grooves of P1 and P3. A different stretched conformation of the ligand was observed for the SAM-II riboswitch (30) (Figure 4*b*). In this structure, SAM aligns along the major groove face of the P2b-L1 triplex and uses all available functional groups for interactions with RNA. In the SAM-III riboswitch (Figure 4*c*), like the SAM-I riboswitch, the bound ligand is bent, but to a lesser extent, so that the methionine moiety is placed alongside the adenine ring, is partially disordered, and is not engaged in hydrogen bonding (65).

The bound extended SAH molecule in the SAH riboswitch structure lies in a cleft created by the minor grooves of P2b and P1 and interacts with RNA using base-specific hydrogen bonding of the adenine moiety and multiple hydrogen bonds involving the homocysteine moiety (24) (Figure 4*d*). Similarities in the recognition of SAM/SAH ligands are limited to stacking of the adenine moiety with RNA bases and the readout of the Hoogsteen edge of adenines by RNA. A common feature of SAM riboswitches that is essential for discrimination against SAH involves electrostatic interactions between the positively charged sulfur moiety andO4 carbonyls of uracils. SAH lacks a methyl group, as well as the positive charge on the sulfur atom, and cannot be substituted by SAM, because of the steric clash between the methyl group and nucleotides of the riboswitch. The critical differences in both overall RNA tertiary organization and ligand recognition observed in the SAM/SAH riboswitch structures illustrate that riboswitches targeting the same or related cellular metabolites have evolved independently.

The three-way junction-based TPP riboswitch structure demonstrates another principle of metabolite recognition (25, 101, 116) (Figure 4*e*). Unlike adenine/guanine riboswitches, TPP does not bind to the junction and instead bridges the middle regions of two helices, which form separate binding pockets for each of TPP's two extremities. The aminopyrimidine moiety binds through base-specific hydrogen-bonding and intercalative stacking interactions, whereas the pyrophosphate moiety forms direct and Mg^{2+}-mediated contacts with RNA (Figure 4*e*). Similar to adenine/guanine riboswitches, TPP ligand-binding stabilizes long-distance tertiary interactions and holds together the junctional region, thereby stabilizing the regulatory helix P1.

The structure of the THF riboswitch reveals one more architectural principle available for metabolite-binding RNAs (39, 118) (Figure 4*f*). This riboswitch adopts a junctional fold in which the three-way junction and long-distance tertiary contacts have switched places to generate the scaffold. Unlike any other single metabolite-sensing aptamer, the *Streptococcus mutans* THF riboswitch binds two ligand molecules (118). The first molecule interacts with

the widened helix adjacent to the remotely positioned three-way junction, thereby stabilizing the junction, whereas the second ligand binds to the minor groove face of the site adjacent to the long-range pseudoknot pairing, apparently stabilizing the pseudoknot and helix P1 (Figure 4*f*). Ligand binding is similar in both sites and, in contrast to many other riboswitches, is characterized by specific recognition of only the small pterin moiety of the ligand, primarily by conserved pyrimidines C53 and U25 near the junction and byU42 andU7 near the pseudoknot (Figure 4*f*). The middle benzoate ring of the first ligand participates in stacking with the guanine base, whereas the terminal glutamate moieties of both ligands, constituting almost one-third of the ligand, appear to not interact with the RNA.

Another structure of the THF riboswitch (39) has captured a conformation that could be considered an intermediate state of riboswitch folding. In this riboswitch from *Eubacterium siraeum*, helix P1 and an adjacent segment participate in intermolecular interactions with a symmetry-related riboswitch molecule. Therefore, the ligand-binding site near the junction is preserved and the putative site in the pseudoknot region appears to be disrupted. Future studies should address whether the *E. siraeum* riboswitch and other THF riboswitches bind to one or two ligand molecules. Inactivation of one binding site in the *S. mutans* riboswitch does not eliminate regulation, while the presence of two sites enhances binding affinity indicative of cooperative binding between two ligand molecules (118).

Most unusually, the FMN riboswitch structure is centered on a six-helix junction and contains domains P2/L2–P6/L6 and P3/L3–P5/L5, which are related by unanticipated approximate twofold symmetry (99) (Figure 4*g*). These domains are stapled together by multiple tertiary interactions within T-loop and A-minor motifs that constitute almost the entire domain structures. FMN is enveloped asymmetrically within the junctional core and is specifically recognized at both its extremities. The pairing of the isoalloxazine ring chromophore with conserved A99 sets off the entrapment of the switching sequence, whereas direct and Mg^{2+}-mediated contacts between the phosphate moiety and RNA increase ligand-binding affinity (Figure 4*g*).

Metallosensors and a Phosphoamino Sugar-Specific Ribozyme

Mg^{2+} cations shield negative charges of the RNA phosphates and assist in the folding of many RNAs. Two distinct RNAs have taken advantage of the RNA-binding ability of Mg^{2+} cations to specifically use them as effectors of the riboswitch-based control of cation-associated transporter genes (17, 19). Insights into the structural principles underlying Mg^{2+}-driven riboswitch control have been provided by the structure of the M-box, the most abundant of two Mg^{2+} sensors (19) (Figure 5*a*). The structure conforms to formation of a junctional architecture and comprises a short hairpin P6 and two long parallel stacks (P2 and P3/P4) connected by a remote junction. The P5/L5 hairpin branches off from the P3/P4 helix and together with the L4 loop forms long-range tertiary contacts that induce P1 helix formation. The tertiary interactions are mediated by four Mg^{2+} cations buried within segments of core 1 area (Figure 5*a*) and apparently require additional cations from core 2 and 3 areas for the alignment of the interacting helices (90, 122). Therefore, the M-box

riboswitch appears to function as a cooperative system dependent on coordination of several divalent cations.

The overall fold of the g*lmS* riboswitch/ribozyme is characterized by three parallel helical stacks and, similar to THF and Mg^{2+} sensors, can be viewed as an architecture containing a junction located remotely from the domain-closing helix P1 (13, 50) (Figure 5*b*). The peripheral RNA domain (P4–P4.1) buttresses a doubly pseudoknotted core that hosts the GlcN6P-binding pocket in the vicinity of the active site. The ligand orients its primary amine toward the labile phosphate linkage of the ribozyme through hydrogen bonds with the ligand sugar moiety and Mg^{2+}-mediated contacts with the phosphate (Figure 5*b*). These structural data along with biochemical experiments suggest that GlcN6P directly participates in RNA cleavage, with its amino group serving as the general acid during cleavage chemistry (13, 20,50, 52, 62, 69).Mg^{2+} cations, usually suspected of involvement in ribozyme catalysis, appear to limit their role to supporting structure formation in the *glmS* riboswitch/ribozyme (37, 48, 96).

STRUCTURAL PRINCIPLES OF METABOLITE RECOGNITION

Riboswitch Architectures

On the basis of the availability of seven riboswitch structures up to 2008, it was proposed that riboswitches be sorted into two distinct types on the basis of binding pocket architectures and conformational effects of ligand binding (75). Type I riboswitches consist of largely preorganized tertiary structures with a single binding pocket and limited ligand-induced conformational adjustments, as observed for the adenine, guanine, and SAM-II riboswitches, as well as the *glmS* ribozyme. Type II riboswitches contain a bipartite binding pocket and experience global conformational changes and adjustments within their ligand-binding pockets, as observed for the TPP, SAM-I, and Mg^{2+} sensors. Riboswitch structures determined since 2008 can also be grouped according to this classification, although the distinction between the two types is less apparent for some riboswitches. For instance, the THF sensor adopts compact ligand-binding pockets as observed for type I riboswitches but, similar to type II riboswitches, appears to require a large conformational change for formation of the long-distance pseudoknot interactions that stabilize the regulatory helix P1 (39). Other riboswitch structures, with the exception of the FMN riboswitch (99), better fit the description of type I riboswitches.

A dissection of almost three dozen currently available riboswitch structures has revealed several common structural trends. First, most riboswitches follow the general architectural principles employed by other large cellular RNAs and are built by coaxial helical stacks or their bundles are connected by junctional regions and pseudoknots. The three-way junctions are most common among riboswitch scaffolds and are present in riboswitches with more complex architectures. Second, helical elements in many riboswitches are organized with recurrent structural RNA motifs observed in other RNAs. These motifs range from small elements, such as A-minor triples (82), to more complex arrangements, such as kink-turn (51) and T-loop (53, 78) motifs, which serve as modular building blocks for larger domains of greater structural complexity, such as a T-loop PK domain (42) found in the FMN riboswitch (99) and 23S ribosomal RNA(42).Despite the similarity of the T-loop PK

domains, riboswitch and rRNA domains differ functionally. In the riboswitch, the pair of T-loop PK domains serve as molecular staples to shape the FMN-binding pocket, whereas in rRNA they form stable platforms for interactions with proteins and other rRNA segments.

Third, the global folds are typically locked by tertiary long-distance interactions that are either induced or stabilized by ligand binding. These interactions, often formed with recurrent structural motifs, reinforce RNA folds and are important for ligand binding and riboswitch response. Fourth, most ligand-binding pockets are located in close proximity to switching sequences. Because alternative pairing of the switching sequences depends on the presence of ligand, the close juxtaposition of the bound ligand and the element responsible for riboswitch response facilitates the transduction of the metabolic signal to the expression platform. Finally, practically all riboswitches demonstrate a dependence on metal cations for their function. Similar to other cellular RNAs, structural studies have revealed multiple bound metal cations distributed within the riboswitch scaffolds that are apparently involved in riboswitch folding and stabilization of the RNA conformation. Some metals that are found in the ligand-binding pockets carry out a specific task, such as neutralization of negative charges of the carboxylate and phosphate moieties of riboswitch ligands (12, 13,25, 50, 54, 98, 99, 101, 104, 105, 116). These Mg^{2+} and K^{+} cations have parallels with cations observed at the intermolecular interfaces in the structures of RNA-protein and metabolite-protein complexes. Nevertheless, riboswitch RNAs tend to utilize cations for mediation of the intermolecular contacts more often than observed for proteins (98, 101).

The emergence of novel riboswitch structures has uncovered the presence of two general architectures for junctional riboswitches on the basis of the relative position of the junction, long-distance tertiary contacts, and the switching sequence. In most riboswitches, which could be ascribed to the first regular group, junctional regions either sequester a regulatory element or contribute to the base-pairing of a switching sequence within the adjacent P1 helix, upon binding of the ligand to the junction or to regions about the junction (Figure 6*a*,*b*). Such junctional folds are typically strengthened by long-range tertiary interactions between peripheral elements, as in the adenine/guanine and TPP riboswitches. For riboswitches of the second group, the long-distance tertiary interactions and junctional region switch locations, so that the junction is positioned remotely to the regulatory helix, whereas tertiary contacts are directly involved in the buildup of the regulatory helix P1 (Figure 6*c*). This alternate inverted junctional architecture has become apparent in the SAM-I riboswitch (74) but is more pronounced in the Mg^{2+} (19) and THF (39) sensors, which contain a junction situated further from helix P1. As was observed for the adenine and TPP riboswitches from the first group, riboswitches with the inverted architecture also position their ligands in proximity to helix P1 and closely to the remote junctional regions (Figure 6*c*,*d*). The inverted junctional architecture may be ascribed to the *glmS* ribozyme, although the stabilization of the closing helix P1 in this RNA does not lead to functional consequences.

Trends in Metabolite Recognition

Early riboswitch structures have revealed that riboswitches typically recognize most functional groups of their cognate ligands. This observation is consistent with a common

view that the riboswitch response must be triggered by one particular compound, and the recognition of several specific ligand determinants ensures the precise selection of a correct ligand from a pool of many similar compounds. Such high riboswitch specificity was correlated with tight binding pockets found in several riboswitches, such as adenine and lysine sensors, which almost completely encapsulated their ligands, leaving 2–15% of the ligand surface accessible to solvent. However, high specificity and affinity of metabolite recognition can also be achieved by in vitro–selected RNAs with smaller buried ligand surfaces of about 70% of the total ligand surfaces (26).Not surprisingly, recent structures have shown that riboswitches can also bury a similar percentage of their ligand surfaces; the THF riboswitch is an extreme case—about half of the ligand is accessible to solvent (39). Such riboswitches either form compact semiopen binding pockets, as in the THF and SAH riboswitches, or contain bipartite binding pockets, as in the TPP riboswitch.

Somewhat surprising was the finding that some riboswitches, for instance, SAM-III, c-di-GMP-II, TFH, and TPP riboswitches, do not take advantage of all available functional groups. There are several possible explanations for this phenomenon. First, a limited number of ligand chemical groups can be sufficient for specific recognition, as in the TPP riboswitch. Second, the size of the RNA-ligand interface typically correlates with the ligand-binding affinity (26); therefore, some riboswitches could have evolved to respond to higher ligand concentrations. Third, riboswitches may be triggered by a family of similar ligands, as has been suggested for the THF and preQ$_1$ riboswitches (4, 39, 44, 97).

Along with this proposal is a recent in vivo kinetics study that showed the activation and inhibition of the *glmS* ribozyme by analogs of the cognate ligand GlcN6P, glucosamine and glucose-6-phosphate, respectively, suggesting that riboswitches integrate information from an array of chemical signals based on the metabolic state of the cell (124).The noncognate compounds triggering the riboswitch response may not be the best binders but, at sufficient intercellular concentration, can outcompete the cognate ligands for riboswitch binding.

Structural studies have revealed that ligand-binding pockets of riboswitches can accommodate a variety of compounds resembling the corresponding cognate metabolites. This could be achieved by moving the entire sensing helix, as in the case of the TPP riboswitch recognizing thiamine monophosphate, a TPP analog that lacks one phosphate moiety (25). Alternatively, a smaller structural element or a few nucleotides can be shifted, as in the dG riboswitch bound to dGMP, for which a ~4,000-fold-weaker binding affinity is associated with the extra phosphatemoiety (88), or in the FMN riboswitch bound to riboflavin, where a ~1,000-fold-reduced binding affinity is associated with the nonphosphorylated precursor of FMN(99). Even riboswitches with seemingly rigid pockets, such as the lysine riboswitch, are capable of making small adjustments to fit additional chemical groups (98).

The inherent plasticity of the ligand-binding pockets explains the interactions with antimicrobial compounds that mimic cellular metabolites. Limited and localized conformational changes have been observed in antibiotic-bound riboswitch structures such as the TPP riboswitch bound to pyrithiamine pyrophosphate (115), the FMN riboswitch bound to roseoflavin (99), and the lysine riboswitch bound to near-cognate compounds (98).

Recent successes in the structure-guided identification of novel compounds that fit tight purine-binding pockets (18) and target riboswitches in clinically relevant bacterial strains (46, 76) will undoubtedly encourage future structure-guided development of antimicrobials that take into account the flexibility of riboswitch-binding pockets.

The inherent plasticity of the ligand-binding site was also a key facet in the re-engineering of riboswitch specificity, whereby a modified adenine riboswitch responded to a nonnatural ligand (22). This approach could allow future development of new small-molecule responsive regulatory systems for biotechnology applications on the basis of the existing riboswitch scaffolds.

RIBOSWITCH FOLDING

The crystal structures of metabolite-bound riboswitch domains have typically revealed a frozen snapshot of one riboswitch state among several states that define the pathway. Such single static pictures provide critical but somewhat limited information on the entire sequence of events involved in riboswitch-mediated gene regulation and require complementary studies of riboswitch folding and dynamics to provide a more comprehensive understanding of the molecular mechanism underlying riboswitch function.

Global Folding Pathways

Riboswitch-dependent gene expression modulation can be divided into three phases (110):

- **a.** folding phase, during which a metabolite-sensing domain folds into its initial structure;
- **b.** sensing phase, during which the sensor evaluates the presence of the cognate ligand; and
- **c.** regulatory phase, during which the sensor adopts a conformation that affects gene expression.

The first phase, the formation of the initial riboswitch conformation, is detrimental to riboswitch function. This step proceeds under strict temporal constraints imposed by the transcription machinery and should at the end produce an RNA conformation that recognizes the cognate ligand and that appears capable of guiding riboswitch folding to an alternative ligand-free route.

Studies of the folding phase are typically based on structural information for metabolite-sensing domains and, because of technical challenges, rely on denaturation and refolding approaches that do not take into account cotranscriptional folding. These studies often compare ligand-unbound and ligand-bound states and therefore involve the metabolite-sensing/metabolite-binding phase to identify conformational transitions upon ligand binding. The folding process has been monitored by a range of approaches on several riboswitches. The biochemical methods, such as in-line probing (106), SHAPE (71), and hydroxyl radical and nuclease footprinting, have analyzed structure-dependent accessibility of nucleotides to different probes for various riboswitch states, as well as conditions that affect conformational stability, for instance, high temperature or lack of metal cations (38). Among

available biophysical methods (1), a vast amount of information has been obtained by fluorescence resonance energy transfer (FRET) and single-molecule FRET (smFRET) (61), the 2-aminopurine (2AP) fluorescence approach (2ApFold) (36), single-molecule force spectroscopy (32), SAXS (63), and various NMR spectroscopic techniques (11, 58, 83, 84).

The folding pathway of adenine riboswitches has been investigated in great detail by a large variety of methods. Initial smFRET experiments using the *Bacillus subtilis pbuE* RNA construct with donor and acceptor fluorophores placed in the L2 and L3 loops exhibited a low FRET signal in the absence of Mg^{2+} and ligand (61).The addition of Mg^{2+} increased the FRET signal, suggesting close positioning of fluorophores that most likely reflect formation of tertiary L2–L3 interactions (Figure 2*a*), which are further stabilized by adenine binding. A folding trajectory of the *B. subtilis pbuE* adenine riboswitch investigated by single-molecule force spectroscopy revealed a five-staged folding of the RNA (32) (Figure 7*a*). The process begins with folding of helix P2, followed by formation of helix P3, tertiary L2–L3 interactions, and finally organization of helix P1. The folded state can be reached in the absence of adenine; however, adenine binding stabilized this state by 4 kcal mol^{-1} and raised the energy barrier for leaving the state. The Mg^{2+}-facilitated formation of tertiary loop-loop interactions in the *add* RNA precedes organization of the least-stable helix P1, which is formally a secondary structure element; therefore, folding of this RNA species can be considered sequential and not hierarchical, thereby more resembling cotranscriptional folding. Biochemical data (109) and NMR studies (11, 58) are in general agreement with the pathway proposed by force spectroscopy. Interestingly, the folding trajectory of the closely related *Vibrio vulnificus add* adenine riboswitch deviates from the *pbuE* RNA folding in the initial stage and reveals the formation of helix P3 prior to P2 (81), thus highlighting effects of small sequence changes on the folding pathway.

In contrast to the adenine sensor, the global fold of the SAM-II riboswitch, another type I riboswitch, appears to critically depend on the ligand binding as analyzed by NMR, FRET, and smFRET (35).The free riboswitch is highly dynamic and, in the absence of Mg^{2+} and SAM, adopts a stem-loop conformation with a flexible RBS containing the unpaired 3′ segment (Figure 7*b*). Addition of Mg^{2+} stabilizes the P1–L3 interactions and significantly populates the conformation with a long-distance pseudoknot involving pairing labeled P2a. SAM captures this ligand-binding competent conformation and stabilizes the pseudoknot fold by inducing additional tertiary pairing labeled P2b.

Similar to the adenine and SAM-II riboswitches, folding of the larger SAM-I sensor, which belongs to type II riboswitches, involves Mg^{2+}-induced conformational rearrangements of the free riboswitch, but on a larger scale (38). An array of techniques, including comparative native gel-electrophoresis, FRET, smFRET, and 2AP fluorescence, demonstrated that the initially unfolded Y-shaped molecule, whose secondary structure elements are preformed but positioned arbitrarily with respect to each other, adopts a more compact conformation upon addition of Mg^{2+} (Figure 7*c*). In this conformer, P2b participates in pseudoknot formation, whereas P2 stacks on P3, thus closely positioning P3 to P1. SAM binding to this preorganized conformation produces the folded state, which is characterized by stacked P1 and P4 helices and rotated helix P1.

The folding models obtained to date demonstrate a diversity of folding strategies adopted by several distinct riboswitches. This variety is not surprising given the diversity of riboswitch structures. Nevertheless, most models illustrate the importance of Mg^{2+}-dependent tertiary contact formation prior to ligand binding, as the tertiary structure preorganizes the ligand-binding pocket and sets the stage for ligand binding.

Ligand Sensing and Folding

Following the folding stage, the metabolite-sensing domain must specifically select the cognate ligand and make conformational adjustments that facilitate the regulatory response. Encapsulation of metabolites within riboswitches, revealed by the first riboswitch structures (7, 102), immediately implied the dynamic nature of the ligand-binding pocket required to provide access to the interior of the pocket, followed by the pocket closure. Such recognition could be described in terms of the induced-fit hypothesis, which posits that ligand binding drives the free state of a receptor to a new conformation that is more complementary to the ligand (Figure 8*a*). On the other hand, some metabolites bind in semiopen pockets that might not require major rearrangements for metabolite access to the pocket (39). Such a binding mechanism can be described by the lock-and-key hypothesis, which states that ligand binding is driven by inherent complementarities between the ligand and the target (Figure 8*b*). In recent years, the dynamic nature of biomolecules has led to the concept of conformational selection, which postulates the preexistence of multiple target conformations, including ligand-binding-competent conformation(s) selected by the ligand from the dynamic ensemble (for review, see Reference 9) (Figure 8*c*). In this context, the lock-and-key model is a case of conformational selection when the ligand binds to the lowest-energy conformer.

To understand the molecular recognition concepts with applications to riboswitches, significant efforts have been devoted to the determination of riboswitch structures in the free form. Surprisingly, the ligand-unbound structures exhibit high similarity to the bound structures, including several examples of pockets with blocked access. The structures of the free and bound states were practically identical, as in the lysine riboswitch (29, 98) and the *glmS* ribozyme (50), with slight differences observed in the ligand-binding pockets for the glycine (40) and THF (39) riboswitches. Small differences were also observed for pocket-neighboring regions, as in the $preQ_1$ (44) and FMN (120) riboswitches, and with internal residues placed instead of ligands, as in the SAM-I (110) and $preQ_1$ (44) riboswitches. However, regardless of the extent of similarity between ligand-bound and ligand-unbound crystal structures, the conformational selection model appears to prevail for ligand recognition and binding by riboswitches according to solution data.

The study on the SAM-I riboswitch has demonstrated that the ligand-unbound and ligand-bound structures do not adequately describe SAXS solution data. Rather, they have to be deconvoluted using an ensemble of structures to optimize for the best fit (110). The SAM-I riboswitch samples multiple conformations via a scissoring motion between P1 and P3, in agreement with fast interconversions observed by smFRET in the unfolded and Mg^{2+}-bound states (Figure 7*c*). The ligand then binds to the bound-like state and shifts the RNA population to the homogeneous fully structured state.

Similar to the SAM-I riboswitch, near-bound states and conformational heterogeneity have also been detected in other riboswitch systems, and the conformational selection model appears to be valid for several riboswitches (120), including the SAM-I counterpart SAM-II (35) and SAM-III (129) riboswitches. The hallmark of the conformation selection model, a near-bound conformation, may be tricky to detect in solution because the level of structural preorganization in the major conformers of the free state differs for various riboswitches (5). Some riboswitches, such as the TPP (2, 25, 56) and c-di-GMP-I (54) riboswitches, sample large conformational space and their ligand-unbound and ligand-bound conformations are markedly distinct, thereby appealing to the induced-fit model. Other riboswitches, such as adenine and guanine riboswitches, are mainly pre-folded. Their conformationally dynamic segments are predominantly restricted to the junctional core regions J1/2 and J2/3 (10, 31,61, 92, 109), suggesting a binding model that can be described as a combined predetermined induced-fit mechanism (83, 86). Heterogenic and dynamic purine binding restricted to the ligand-binding pocket has been observed by femtosecond time-resolved fluorescence spectroscopy (43). These observations in principle support the binding mechanism and are in line with the conformational selection model for the adenine and guanine riboswitches. The *glmS* ribozyme appears to be even more preorganized, with structural (13, 50), hydroxyl radical footprinting, UV cross-linking (37), FRET, and nuclease and chemical footprinting (117) studies establishing that it does not adjust its conformation upon ligand binding.

The adaptation of a fully bound state requires conformational changes in the RNA, such as closure of the binding pocket, indicating synergism between conformational capture and induced-fit modes of ligand binding. Induced-fit may also play a critical role in the regulatory response driven by stabilization and/or formation of the regulatory helix P1 in riboswitches that do not directly sequester RBS. Although basic structural principles of helix P1 stabilization are understood, the mechanics of the process and related questions, such as the extent of helix preformation that defines a threshold of thermodynamic stability and may contribute to the affinity of the ligand, require further scrutiny. Because nucleotides of helix P1 are often involved in ligand-binding pocket formation, helix P1 may need to be preformed, at least transiently, for metabolite recognition. Alternately, the ligand was proposed to interact with the riboswitch prior to helix formation (41). The early recognition of the ligand may be essential to minimize binding time and guarantee the formation of a stable ligand-RNA complex in order to trigger the formation of the ligand-bound conformation in the expression platform and provide the correct regulatory response.

Kinetic Versus Thermodynamic Control

Can the conformation of riboswitches shift from one state to another, thereby switching gene expression from on to off and vice versa? In bacteria, mRNA turnover is high and a synthesized untranslated mRNA may not survive sufficiently long to sense a change in the environment. Nevertheless, such a possibility does exist, and in the case of riboswitches that operate at the translational level, one could imagine a thermodynamic equilibrium between interconverting riboswitch structures whose populations are shifted by interactions with ligand. In this scenario, the ligand should be able to bind to the fully transcribed riboswitch, as was shown for the *V. vulnificus add* adenine riboswitch (92). This riboswitch was

suggested to fold predominantly into the repressor fold that is in equilibrium with the ligand-binding-competent structure (Figure 9*a*). Upon adenine binding, the equilibrium is shifted toward the thermodynamically favorable ligand-bound conformation with organized helix P1, which breaks the formation of the RBS-sequestering stem and makes the RBS and start codon accessible for ribosome binding (59, 92). Thus, the thermodynamically controlled *V. vulnificus add* adenine riboswitch appears to fulfill the expectation for a true regulatory switch.

Riboswitches that operate by the transcription termination mechanism obviously cannot reverse the regulation when transcription was terminated prior to the synthesis of the coding sequence. However, the coexistence of two competing transcription antiterminator and terminator stem-loop structures in the expression platform and the ligand-induced shift of the ensemble toward the terminator was revealed by NMR and 2ApFold approaches in the *F. nucleatum* preQ$_1$ riboswitch (93). If the RNA polymerase pauses long enough after transcription of the antiterminator stem-loop to sense the ligand-induced shift toward the terminator stem-loop, the thermodynamic control of transcription termination may also occur in vivo.

Most riboswitches that operate via transcription termination mechanism do not reach thermodynamic equilibrium with their ligands. Paradoxically, initial observations revealed a requirement for higher ligand concentration to elicit a 50% transcription termination yield relative to the apparent K_D value, a ligand concentration necessary to engage 50% of RNA in complex formation at equilibrium. This discrepancy was interpreted in terms of the kinetic response: In some riboswitches the RNA polymerase arrives at the termination decision point before the ligand and the sensing domain can reach binding equilibrium. Therefore, a higher metabolite concentration is needed to ensure ligand binding and triggering the formation of the appropriate downstream regulatory element (127, 128). In this regard, riboswitches under kinetic control, such as the *B. subtilis* FMN (128) and *B. subtilis pbuE* adenine (59, 127) riboswitches, are not true switches and function more like molecular fuses (128) (Figure 9*b*). The choice of the thermodynamic or kinetic regime adopted by a riboswitch depends on a multitude of factors, such as the rate of RNA folding, the transcription rate, the ligand association/dissociation rates, and the cellular concentration of the ligand, among others. For many riboswitches, association/dissociation equilibrium time is in the seconds range (135), comparable to the riboswitch transcription time if the polymerase rate approximates 50 nt s^{-1}. Delays can be introduced by transcriptional pausing when riboswitch folding and ligand binding are slower than the transcriptional rate (128).

CONCLUDING REMARKS

Almost a decade of intensive studies has revealed the large diversity of riboswitches and related sensors of physical and chemical cues. This diversity accounts for the multitude of structural principles utilized by riboswitches to make high-precision RNA sensors and effective responders that rival protein-based genetic circuits in bacteria. Structural studies have in turn facilitated detailed biochemical and biophysical characterization of the ligand recognition and mechanisms of riboswitch function while revealing common features with other RNA- and protein-ligand systems. Future studies will aim to utilize ligand recognition

principles and riboswitch mechanics to control gene expression via modified genetic systems and designer ligands.

Acknowledgments

Funding for this work was provided by the New York University start-up grant (A.S.) and NIH grant GM66354 (D.J.P.).

Glossary

RBS	ribosome-binding site or Shine-Dalgarno sequence that facilitates ribosome binding to bacterial mRNAs by pairing the 16S ribosomal RNA with mRNAs
Pseudoknot	a tertiary element of RNA secondary structure involving base-pairing between a loop and a complementary sequence outside the loop
Kink-turn motif	sharply bent internal RNA loop flanked by C–G and G·A base pairs, with an A-minor interaction between two helical stems
Small-angle X-ray scattering (SAXS)	a method that provides a measure of the global RNA conformation in solution
H-type pseudoknot	a pseudoknot formed between nucleotides in a hairpin loop (coded H) and a single-stranded region
LL-type pseudoknot	a pseudoknot variant that involves a pairing between an internal loop and a hairpin-containing loop
A-minor motif	an RNA motif that involves interactions between the minor groove edges of an adenine and a Watson-Crick base pair
T-loop motif	a uridine-containing RNA loop flanked by a noncanonical U·A base pair stacked on one side with a Watson-Crick base pair
In-line probing	RNA-probing technique that relies on the inherent instability of the phosphodiester backbone in flexible RNA regions
Selective 2′-hydroxyl acylation analyzed by primer extension (SHAPE)	a technique that probes RNA flexible regions by a modification of 2′-hydroxyls with *N*-methylisatoic anhydride
FRET	Förster resonance energy transfer dependent on energy transfer between two closely positioned fluorophores in bulk experiments
smFRET	single-molecule version of FRET experiments
2ApFold	an approach to study RNA folding dependent on quenching of 2-aminopurine fluorescence as a result of stacking interactions

Single-molecule force spectroscopy	an approach to study RNA folding that monitors extension of a single RNA molecule upon application of force to its ends
Hierarchical RNA folding	a concept suggesting formation of secondary structure elements followed by formation of tertiary interactions
Comparative native gel-electrophoresis	a hydrodynamic method that correlates changes in RNA mobility with relative orientation of riboswitch helices
K_D	dissociation constant

LITERATURE CITED

1. Al-Hashimi HM, Walter NG. RNA dynamics: It is about time. Curr. Opin. Struct. Biol. 2008; 18:321–329. [PubMed: 18547802]
2. Ali M, Lipfert J, Seifert S, Herschlag D, Doniach S. The ligand-free state of the TPP riboswitch: a partially folded RNA structure. J. Mol. Biol. 2010; 396:153–165. [PubMed: 19925806]
3. Ames TD, Breaker RR. Bacterial aptamers that selectively bind glutamine. RNA Biol. 2011; 8:82–89. [PubMed: 21282981]
4. Ames TD, Rodionov DA, Weinberg Z, Breaker RR. A eubacterial riboswitch class that senses the coenzyme tetrahydrofolate. Chem. Biol. 2010; 17:681–685. [PubMed: 20659680]
5. Baird NJ, Ferre-D'Amare AR. Idiosyncratically tuned switching behavior of riboswitch aptamer domains revealed by comparative small-angle X-ray scattering analysis. RNA. 2010; 16:598–609. [PubMed: 20106958]
6. Baker JL, Sudarsan N, Weinberg Z, Roth A, Stockbridge RB, Breaker RR. Widespread genetic switches and toxicity resistance proteins for fluoride. Science. 2012; 335:233–235. [PubMed: 22194412]
7. Batey RT, Gilbert SD, Montange RK. Structure of a natural guanine-responsive riboswitch complexed with the metabolite hypoxanthine. Nature. 2004; 432:411–415. [PubMed: 15549109]
8. Bocobza SE, Aharoni A. Switching the light on plant riboswitches. Trends Plant Sci. 2008; 13:526–533. [PubMed: 18778966]
9. Boehr DD, Nussinov R, Wright PE. The role of dynamic conformational ensembles in biomolecular recognition. Nat. Chem. Biol. 2009; 5:789–796. [PubMed: 19841628]
10. Brenner MD, Scanlan MS, Nahas MK, Ha T, Silverman SK. Multivector fluorescence analysis of the *xpt* guanine riboswitch aptamer domain and the conformational role of guanine. Biochemistry. 2010; 49:1596–1605. [PubMed: 20108980]
11. Buck J, Furtig B, Noeske J, Wohnert J, Schwalbe H. Time-resolved NMR methods resolving ligand-induced RNA folding at atomic resolution. Proc. Natl. Acad. Sci. USA. 2007; 104:15699–15704. [PubMed: 17895388]
12. Butler EB, Xiong Y, Wang J, Strobel SA. Structural basis of cooperative ligand binding by the glycine riboswitch. Chem. Biol. 2011; 18:293–298. [PubMed: 21439473]
13. Cochrane JC, Lipchock SV, Strobel SA. Structural investigation of the GlmS ribozyme bound to its catalytic cofactor. Chem. Biol. 2007; 14:97–105. [PubMed: 17196404]
14. Collins JA, Irnov I, Baker S, Winkler WC. Mechanism of mRNA destabilization by the glmS ribozyme. Genes. Dev. 2007; 21:3356–3368. [PubMed: 18079181]
15. Corbino KA, Barrick JE, Lim J, Welz R, Tucker BJ, et al. Evidence for a second class of *S*-adenosylmethionine riboswitches and other regulatory RNA motifs in alpha-proteobacteria. Genome Biol. 2005; 6:R70. [PubMed: 16086852]
16. Correll CC, Freeborn B, Moore PB, Steitz TA. Metals, motifs, and recognition in the crystal structure of a 5S rRNA domain. Cell. 1997; 91:705–712. [PubMed: 9393863]
17. Cromie MJ, Shi Y, Latifi T, Groisman EA. An RNA sensor for intracellular Mg^{2+} Cell. 2006; 125:71–84. [PubMed: 16615891]

18. Daldrop P, Reyes FE, Robinson DA, Hammond CM, Lilley DM, et al. Novel ligands for a purine riboswitch discovered by RNA-ligand docking. Chem. Biol. 2011; 18:324–335. [PubMed: 21439477]
19. Dann CE 3rd, Wakeman CA, Sieling CL, Baker SC, Irnov I, et al. Structure and mechanism of a metal-sensing regulatory RNA. Cell. 2007; 130:878–892. [PubMed: 17803910]
20. Davis JH, Dunican BF, Strobel SA. *glmS* riboswitch binding to the glucosamine-6-phosphate α-anomer shifts the pK_a toward neutrality. Biochemistry. 2011; 50:7236–7242. [PubMed: 21770472]
21. Delfosse V, Bouchard P, Bonneau E, Dagenais P, Lemay JF, et al. Riboswitch structure: an internal residue mimicking the purine ligand. Nucleic Acids Res. 2010; 38:2057–2068. [PubMed: 20022916]
22. Dixon N, Duncan JN, Geerlings T, Dunstan MS, McCarthy JE, et al. Reengineering orthogonally selective riboswitches. Proc. Natl. Acad. Sci. USA. 2010; 107:2830–2835. [PubMed: 20133756]
23. Edwards AL, Batey RT. A structural basis for the recognition of 2′-deoxyguanosine by the purine riboswitch. J. Mol. Biol. 2009; 385:938–948. [PubMed: 19007790]
24. Edwards AL, Reyes FE, Heroux A, Batey RT. Structural basis for recognition of *S*-adenosylhomocysteine by riboswitches. RNA. 2010; 16:2144–2155. [PubMed: 20864509]
25. Edwards TE, Ferre-D'Amare AR. Crystal structures of the thi-box riboswitch bound to thiamine pyrophosphate analogs reveal adaptive RNA-small molecule recognition. Structure. 2006; 14:1459–1468. [PubMed: 16962976]
26. Edwards TE, Klein DJ, Ferre-D'Amare AR. Riboswitches: small-molecule recognition by gene regulatory RNAs. Curr. Opin. Struct. Biol. 2007; 17:273–279. [PubMed: 17574837]
27. Epshtein V, Mironov AS, Nudler E. The riboswitch-mediated control of sulfur metabolism in bacteria. Proc. Natl. Acad. Sci. USA. 2003; 100:5052–5056. [PubMed: 12702767]
28. Fuchs RT, Grundy FJ, Henkin TM. The S_{MK} box is a new SAM-binding RNA for translational regulation of SAM synthetase. Nat. Struct. Mol. Biol. 2006; 13:226–233. [PubMed: 16491091]
29. Garst AD, Heroux A, Rambo RP, Batey RT. Crystal structure of the lysine riboswitch regulatory mRNA element. J. Biol. Chem. 2008; 283:22347–22351. [PubMed: 18593706]
30. Gilbert SD, Rambo RP, Van Tyne D, Batey RT. Structure of the SAM-II riboswitch bound to *S*-adenosylmethionine. Nat. Struct. Mol. Biol. 2008; 15:177–182. [PubMed: 18204466]
31. Gilbert SD, Stoddard CD, Wise SJ, Batey RT. Thermodynamic and kinetic characterization of ligand binding to the purine riboswitch aptamer domain. J. Mol. Biol. 2006; 359:754–768. [PubMed: 16650860]
32. Greenleaf WJ, Frieda KL, Foster DA, Woodside MT, Block SM, et al. Direct observation of hierarchical folding in single riboswitch aptamers. Science. 2008; 319:630–633. [PubMed: 18174398]
33. Grundy FJ, Henkin TM. tRNA as a positive regulator of transcription antitermination in *B. subtilis*. Cell. 1993; 74:475–482. [PubMed: 8348614]
34. Grundy FJ, Lehman SC, Henkin TM. The L box regulon: lysine sensing by leader RNAs of bacterial lysine biosynthesis genes. Proc. Natl. Acad. Sci. USA. 2003; 100:12057–12062. [PubMed: 14523230]
35. Haller A, Rieder U, Aigner M, Blanchard SC, Micura R. Conformational capture of the SAM-II riboswitch. Nat. Chem. Biol. 2011; 7:393–400. [PubMed: 21532598]
36. Haller A, Soulière MF, Micura R. The dynamic nature of RNA as key to understanding riboswitch mechanisms. Acc. Chem. Res. 2011; 44:1339–1348. [PubMed: 21678902]
37. Hampel KJ, Tinsley MM. Evidence for preorganization of the *glmS* ribozyme ligand binding pocket. Biochemistry. 2006; 45:7861–7871. [PubMed: 16784238]
38. Heppell B, Blouin S, Dussault AM, Mulhbacher J, Ennifar E, et al. Molecular insights into the ligand-controlled organization of the SAM-I riboswitch. Nat. Chem. Biol. 2011; 7:384–392. [PubMed: 21532599]
39. Huang L, Ishibe-Murakami S, Patel DJ, Serganov A. Long-range pseudoknot interactions dictate the regulatory response in the tetrahydrofolate riboswitch. Proc. Natl. Acad. Sci. USA. 2011; 108:14801–14806. [PubMed: 21873197]

40. Huang L, Serganov A, Patel DJ. Structural insights into ligand recognition by a sensing domain of the cooperative glycine riboswitch. Mol. Cell. 2010; 40:774–786. [PubMed: 21145485]
41. Huang W, Kim J, Jha S, Aboul-ela F. A mechanism for *S*-adenosyl methionine assisted formation of a riboswitch conformation: a small molecule with a strong arm. Nucleic Acids Res. 2009; 37:6528–6539. [PubMed: 19720737]
42. Jaeger L, Verzemnieks EJ, Geary C. The UA_handle: a versatile submotif in stable RNA architectures. Nucleic Acids Res. 2009; 37:215–230. [PubMed: 19036788]
43. Jain N, Zhao L, Liu JD, Xia T. Heterogeneity and dynamics of the ligand recognition mode in purine-sensing riboswitches. Biochemistry. 2010; 49:3703–3714. [PubMed: 20345178]
44. Jenkins JL, Krucinska J, McCarty RM, Bandarian V, Wedekind JE. Comparison of a preQ$_1$ riboswitch aptamer in metabolite-bound and free states with implications for gene regulation. J. Biol. Chem. 2011; 286:24626–24637. [PubMed: 21592962]
45. Kang M, Peterson R, Feigon J. Structural insights into riboswitch control of the biosynthesis of queuosine, a modified nucleotide found in the anticodon of tRNA. Mol. Cell. 2009; 33:784–790. [PubMed: 19285444]
46. Kim JN, Blount KF, Puskarz I, Lim J, Link KH, et al. Design and antimicrobial action of purine analogues that bind guanine riboswitches. ACS Chem. Biol. 2009; 4:915–927. [PubMed: 19739679]
47. Kim JN, Roth A, Breaker RR. Guanine riboswitch variants from *Mesoplasma florum* selectively recognize 2′-deoxyguanosine. Proc. Natl. Acad. Sci. USA. 2007; 104:16092–16097. [PubMed: 17911257]
48. Klawuhn K, Jansen JA, Souchek J, Soukup GA, Soukup JK. Analysis of metal ion dependence in *glmS* ribozyme self-cleavage and coenzyme binding. Chembiochem. 2010; 11:2567–2571. [PubMed: 21108273]
49. Klein DJ, Edwards TE, Ferre-D'Amare AR. Cocrystal structure of a class I preQ$_1$ riboswitch reveals a pseudoknot recognizing an essential hypermodified nucleobase. Nat. Struct. Mol. Biol. 2009; 16:343–344. [PubMed: 19234468]
50. Klein DJ, Ferre-D'Amare AR. Structural basis of *glmS* ribozyme activation by glucosamine-6-phosphate. Science. 2006; 313:1752–1756. [PubMed: 16990543]
51. Klein DJ, Schmeing TM, Moore PB, Steitz TA. The kink-turn: a new RNA secondary structure motif. EMBO J. 2001; 20:4214–4221. [PubMed: 11483524]
52. Klein DJ, Wilkinson SR, Been MD, Ferre-D'Amare AR. Requirement of helix P2.2 and nucleotide G1 for positioning the cleavage site and cofactor of the *glmS* ribozyme. J. Mol. Biol. 2007; 373:178–189. [PubMed: 17804015]
53. Krasilnikov AS, Mondragon A. On the occurrence of the T-loop RNA folding motif in large RNA molecules. RNA. 2008; 9:640–643. [PubMed: 12756321]
54. Kulshina N, Baird NJ, Ferre-D'Amare AR. Recognition of the bacterial second messenger cyclic diguanylate by its cognate riboswitch. Nat. Struct. Mol. Biol. 2009; 16:1212–1227. [PubMed: 19898478]
55. Kwon M, Strobel SA. Chemical basis of glycine riboswitch cooperativity. RNA. 2008; 14:25–34. [PubMed: 18042658]
56. Lang K, Rieder R, Micura R. Ligand-induced folding of the *thiM* TPP riboswitch investigated by a structure-based fluorescence spectroscopic approach. Nucleic Acids Res. 2007; 35:5370–5378. [PubMed: 17693433]
57. Lee ER, Baker JL, Weinberg Z, Sudarsan N, Breaker RR. An allosteric self-splicing ribozyme triggered by a bacterial second messenger. Science. 2010; 329:845–848. [PubMed: 20705859]
58. Lee MK, Gal M, Frydman L, Varani G. Real-time multidimensional NMR follows RNA folding with second resolution. Proc. Natl. Acad. Sci. USA. 2010; 107:9192–9197. [PubMed: 20439766]
59. Lemay JF, Desnoyers G, Blouin S, Heppell B, Bastet L, et al. Comparative study between transcriptionally- and translationally-acting adenine riboswitches reveals key differences in riboswitch regulatory mechanisms. PLoS Genet. 2011; 7:e1001278. [PubMed: 21283784]
60. Lemay JF, Lafontaine DA. Core requirements of the adenine riboswitch aptamer for ligand binding. RNA. 2007; 13:339–350. [PubMed: 17200422]

61. Lemay JF, Penedo JC, Tremblay R, Lilley DM, Lafontaine DA. Folding of the adenine riboswitch. Chem. Biol. 2006; 13:857–868. [PubMed: 16931335]
62. Lim J, Grove BC, Roth A, Breaker RR. Characteristics of ligand recognition by a *glmS* self-cleaving ribozyme. Angew. Chem. Int. Ed. Engl. 2006; 45:6689–6693. [PubMed: 16986193]
63. Lipfert J, Das R, Chu VB, Kudaravalli M, Boyd N, et al. Structural transitions and thermodynamics of a glycine-dependent riboswitch from *Vibrio cholerae*. J. Mol. Biol. 2007; 365:1393–1406. [PubMed: 17118400]
64. Loh E, Dussurget O, Gripenland J, Vaitkevicius K, Tiensuu T, et al. A *trans*-acting riboswitch controls expression of the virulence regulator PrfA in *Listeria monocytogenes*. Cell. 2009; 139:770–779. [PubMed: 19914169]
65. Lu C, Smith AM, Fuchs RT, Ding F, Rajashankar K, et al. Crystal structures of the SAM-III/S_{MK} riboswitch reveal the SAM-dependent translation inhibition mechanism. Nat. Struct. Mol. Biol. 2008; 15:1076–1083. [PubMed: 18806797]
66. Mandal M, Boese B, Barrick JE, Winkler WC, Breaker RR. Riboswitches control fundamental biochemical pathways in *Bacillus subtilis* and other bacteria. Cell. 2003; 113:577–586. [PubMed: 12787499]
67. Mandal M, Breaker RR. Adenine riboswitches and gene activation by disruption of a transcription terminator. Nat. Struct. Mol. Biol. 2004; 11:29–35. [PubMed: 14718920]
68. Mandal M, Lee M, Barrick JE, Weinberg Z, Emilsson GM, et al. A glycine-dependent riboswitch that uses cooperative binding to control gene expression. Science. 2004; 306:275–279. [PubMed: 15472076]
69. McCarthy TJ, Plog MA, Floy SA, Jansen JA, Soukup JK, et al. Ligand requirements for *glmS* ribozyme self-cleavage. Chem. Biol. 2005; 12:1221–1226. [PubMed: 16298301]
70. McDaniel BA, Grundy FJ, Artsimovitch I, Henkin TM. Transcription termination control of the S box system: direct measurement of *S*-adenosylmethionine by the leader RNA. Proc. Natl. Acad. Sci. USA. 2003; 100:3083–3088. [PubMed: 12626738]
71. Merino EJ, Wilkinson KA, Coughlan JL, Weeks KM. RNA structure analysis at single nucleotide resolution by selective 2′-hydroxyl acylation and primer extension (SHAPE). J. Am. Chem. Soc. 2005; 127:4223–4231. [PubMed: 15783204]
72. Meyer MM, Roth A, Chervin SM, Garcia GA, Breaker RR. Confirmation of a second natural $preQ_1$ aptamer class in *Streptococcaceae* bacteria. RNA. 2008; 14:685–695. [PubMed: 18305186]
73. Mironov AS, Gusarov I, Rafikov R, Lopez LE, Shatalin K, et al. Sensing small molecules by nascent RNA: a mechanism to control transcription in bacteria. Cell. 2002; 111:747–756. [PubMed: 12464185]
74. Montange RK, Batey RT. Structure of the *S*-adenosylmethionine riboswitch regulatory mRNA element. Nature. 2006; 441:1172–1175. [PubMed: 16810258]
75. Montange RK, Batey RT. Riboswitches: emerging themes in RNA structure and function. Annu. Rev. Biophys. 2008; 37:117–133. [PubMed: 18573075]
76. Mulhbacher J, Brouillette E, Allard M, Fortier LC, Malouin F, et al. Novel riboswitch ligand analogs as selective inhibitors of guanine-related metabolic pathways. PLoS Pathog. 2010; 6:e1000865. [PubMed: 20421948]
77. Mulhbacher J, Lafontaine DA. Ligand recognition determinants of guanine riboswitches. Nucleic Acids Res. 2007; 35:5568–5580. [PubMed: 17704135]
78. Nagaswamy U, Fox GE. Frequent occurrence of the T-loop RNA folding motif in ribosomal RNAs. RNA. 2002; 8:1112–1119. [PubMed: 12358430]
79. Nahvi A, Barrick JE, Breaker RR. Coenzyme B12 riboswitches are widespread genetic control elements in prokaryotes. Nucleic Acids Res. 2004; 32:143–150. [PubMed: 14704351]
80. Nahvi A, Sudarsan N, Ebert MS, Zou X, Brown KL, et al. Genetic control by a metabolite binding mRNA. Chem. Biol. 2002; 9:1043–1049. [PubMed: 12323379]
81. Neupane K, Yu H, Foster DA, Wang F, Woodside MT. Single-molecule force spectroscopy of the add adenine riboswitch relates folding to regulatory mechanism. Nucleic Acids Res. 2011; 39:7677–7687. [PubMed: 21653559]

82. Nissen P, Ippolito JA, Ban N, Moore PB, Steitz TA. RNA tertiary interactions in the large ribosomal subunit: the A-minor motif. Proc. Natl. Acad. Sci. USA. 2001; 98:4899–4903. [PubMed: 11296253]

83. Noeske J, Buck J, Furtig B, Nasiri HR, Schwalbe H, et al. Interplay of 'induced fit' and preorganization in the ligand induced folding of the aptamer domain of the guanine binding riboswitch. Nucleic Acids Res. 2007; 35:572–583. [PubMed: 17175531]

84. Noeske J, Richter C, Grundl MA, Nasiri HR, Schwalbe H, et al. An intermolecular base triple as the basis of ligand specificity and affinity in the guanine- and adenine-sensing riboswitch RNAs. Proc. Natl. Acad. Sci. USA. 2005; 102:1372–1377. [PubMed: 15665103]

85. Nudler E, Mironov AS. The riboswitch control of bacterial metabolism. Trends Biochem. Sci. 2004; 29:11–17. [PubMed: 14729327]

86. Ottink OM, Rampersad SM, Tessari M, Zaman GJ, Heus HA, et al. Ligand-induced folding of the guanine-sensing riboswitch is controlled by a combined predetermined induced fit mechanism. RNA. 2007; 13:2202–2212. [PubMed: 17959930]

87. Park SY, Cromie MJ, Lee EJ, Groisman EA. A bacterial mRNA leader that employs different mechanisms to sense disparate intracellular signals. Cell. 2010; 142:737–748. [PubMed: 20813261]

88. Pikovskaya O, Polonskaia A, Patel DJ, Serganov A. Structural principles of nucleoside selectivity in a 2′-deoxyguanosine riboswitch. Nat. Chem. Biol. 2011; 7:748–755. [PubMed: 21841796]

89. Poiata E, Meyer MM, Ames TD, Breaker RR. A variant riboswitch aptamer class for *S*-adenosylmethionine common in marine bacteria. RNA. 2009; 15:2046–2056. [PubMed: 19776155]

90. Ramesh A, Wakeman CA, Winkler WC. Insights into metalloregulation by M-box riboswitch RNAs via structural analysis of manganese-bound complexes. J. Mol. Biol. 2011; 407:556–570. [PubMed: 21315082]

91. Regulski EE, Moy RH, Weinberg Z, Barrick JE, Yao Z, et al. A widespread riboswitch candidate that controls bacterial genes involved in molybdenum cofactor and tungsten cofactor metabolism. Mol. Microbiol. 2008; 68:918–932. [PubMed: 18363797]

92. Rieder R, Lang K, Graber D, Micura R. Ligand-induced folding of the adenosine deaminase A-riboswitch and implications on riboswitch translational control. Chembiochem. 2007; 8:896–902. [PubMed: 17440909]

93. Rieder U, Kreutz C, Micura R. Folding of a transcriptionally acting preQ$_1$ riboswitch. Proc. Natl. Acad. Sci. USA. 2010; 107:10804–10809. [PubMed: 20534493]

94. Rodionov DA, Vitreschak AG, Mironov AA, Gelfand MS. Regulation of lysine biosynthesis and transport genes in bacteria: yet another RNA riboswitch? Nucleic Acids Res. 2003; 31:6748–6757. [PubMed: 14627808]

95. Roth A, Breaker RR. The structural and functional diversity of metabolite-binding riboswitches. Annu. Rev. Biochem. 2009; 78:305–334. [PubMed: 19298181]

96. Roth A, Nahvi A, Lee M, Jona I, Breaker RR. Characteristics of the glmS ribozyme suggest only structural roles for divalent metal ions. RNA. 2006; 12:607–619. [PubMed: 16484375]

97. Roth A, Winkler WC, Regulski EE, Lee BW, Lim J, et al. A riboswitch selective for the queuosine precursor preQ$_1$ contains an unusually small aptamer domain. Nat. Struct. Mol. Biol. 2007; 14:308–317. [PubMed: 17384645]

98. Serganov A, Huang L, Patel DJ. Structural insights into amino acid binding and gene control by a lysine riboswitch. Nature. 2008; 455:1263–1267. [PubMed: 18784651]

99. Serganov A, Huang L, Patel DJ. Coenzyme recognition and gene regulation by a flavin mononucleotide riboswitch. Nature. 2009; 458:233–237. [PubMed: 19169240]

100. Serganov A, Patel DJ. Ribozymes, riboswitches and beyond: regulation of gene expression without proteins. Nat. Rev. Genet. 2007; 8:776–790. [PubMed: 17846637]

101. Serganov A, Polonskaia A, Phan AT, Breaker RR, Patel DJ. Structural basis for gene regulation by a thiamine pyrophosphate-sensing riboswitch. Nature. 2006; 441:1167–1171. [PubMed: 16728979]

102. Serganov A, Yuan YR, Pikovskaya O, Polonskaia A, Malinina L, et al. Structural basis for discriminative regulation of gene expression by adenine- and guanine-sensing mRNAs. Chem. Biol. 2004; 11:1729–1741. [PubMed: 15610857]
103. Shanahan CA, Gaffney BL, Jones RA, Strobel SA. Differential analog binding by two classes of c-di-GMP riboswitches. J. Am. Chem. Soc. 2011; 133:15578–15592. [PubMed: 21838307]
104. Smith KD, Lipchock SV, Ames TD, Wang J, Breaker RR, et al. Structural basis of ligand binding by a c-di-GMP riboswitch. Nat. Struct. Mol. Biol. 2009; 16:1218–1223. [PubMed: 19898477]
105. Smith KD, Shanahan CA, Moore EL, Simon AC, Strobel SA. Structural basis of differential ligand recognition by two classes of bis-(3′–5′)-cyclic dimeric guanosine monophosphate-binding riboswitches. Proc. Natl. Acad. Sci. USA. 2011; 108:7757–7762. [PubMed: 21518891]
106. Soukup GA, Breaker RR. Relationship between internucleotide linkage geometry and the stability of RNA. RNA. 1999; 5:1308–1325. [PubMed: 10573122]
107. Spinelli SV, Pontel LB, Garcia Vescovi E, Soncini FC. Regulation of magnesium homeostasis in *Salmonella*: Mg^{2+} targets the *mgtA* transcript for degradation by RNase E. FEMS Microbiol. Lett. 2008; 280:226–234. [PubMed: 18248433]
108. Spitale RC, Torelli AT, Krucinska J, Bandarian V, Wedekind JE. The structural basis for recognition of the $PreQ_0$ metabolite by an unusually small riboswitch aptamer domain. J. Biol. Chem. 2009; 284:11012–11016. [PubMed: 19261617]
109. Stoddard CD, Gilbert SD, Batey RT. Ligand-dependent folding of the three-way junction in the purine riboswitch. RNA. 2008; 14:675–684. [PubMed: 18268025]
110. Stoddard CD, Montange RK, Hennelly SP, Rambo RP, Sanbonmatsu KY, et al. Free state conformational sampling of the SAM-I riboswitch aptamer domain. Structure. 2010; 18:787–797. [PubMed: 20637415]
111. Sudarsan N, Barrick JE, Breaker RR. Metabolite-binding RNA domains are present in the genes of eukaryotes. RNA. 2003; 9:644–647. [PubMed: 12756322]
112. Sudarsan N, Hammond MC, Block KF, Welz R, Barrick JE, et al. Tandem riboswitch architectures exhibit complex gene control functions. Science. 2006; 314:300–304. [PubMed: 17038623]
113. Sudarsan N, Lee ER, Weinberg Z, Moy RH, Kim JN, et al. Riboswitches in eubacteria sense the second messenger cyclic di-GMP. Science. 2008; 321:411–413. [PubMed: 18635805]
114. Sudarsan N, Wickiser JK, Nakamura S, Ebert MS, Breaker RR. An mRNA structure in bacteria that controls gene expression by binding lysine. Genes Dev. 2003; 17:2688–2697. [PubMed: 14597663]
115. Thore S, Frick C, Ban N. Structural basis of thiamine pyrophosphate analogues binding to the eukaryotic riboswitch. J. Am. Chem. Soc. 2008; 130:8116–8117. [PubMed: 18533652]
116. Thore S, Leibundgut M, Ban N. Structure of the eukaryotic thiamine pyrophosphate riboswitch with its regulatory ligand. Science. 2006; 312:1208–1211. [PubMed: 16675665]
117. Tinsley RA, Furchak JR, Walter NG. *Trans*-acting *glmS* catalytic riboswitch: locked and loaded. RNA. 2007; 13:468–477. [PubMed: 17283212]
118. Trausch JJ, Ceres P, Reyes FE, Batey RT. The structure of a tetrahydrofolate-sensing riboswitch reveals two ligand binding sites in a single aptamer. Structure. 2011; 19:1413–1423. [PubMed: 21906956]
119. Tremblay R, Lemay JF, Blouin S, Mulhbacher J, Bonneau E, et al. Constitutive regulatory activity of an evolutionarily excluded riboswitch variant. J. Biol. Chem. 2011; 286:27406–27415. [PubMed: 21676871]
120. Vicens Q, Mondragón E, Batey RT. Molecular sensing by the aptamer domain of the FMN riboswitch: a general model for ligand binding by conformational selection. Nucleic Acids Res. 2011; 39:8586–8598. [PubMed: 21745821]
121. Wachter A. Riboswitch-mediated control of gene expression in eukaryotes. RNA Biol. 2010; 7:67–76. [PubMed: 20009507]
122. Wakeman CA, Ramesh A, Winkler WC. Multiple metal-binding cores are required for metalloregulation by M-box riboswitch RNAs. J. Mol. Biol. 2009; 392:723–735. [PubMed: 19619558]

123. Wang JX, Breaker RR. Riboswitches that sense *S*-adenosylmethionine and *S*-adenosylhomocysteine. Biochem. Cell Biol. 2008; 86:157–168. [PubMed: 18443629]

124. Watson PY, Fedor MJ. The *glmS* riboswitch integrates signals from activating and inhibitory metabolites in vivo. Nat. Struct. Mol. Biol. 2011; 18:359–363. [PubMed: 21317896]

125. Weinberg Z, Regulski EE, Hammond MC, Barrick JE, Yao Z, et al. The aptamer core of SAM-IV riboswitches mimics the ligand-binding site of SAM-I riboswitches. RNA. 2008; 14:822–828. [PubMed: 18369181]

126. Weinberg Z, Wang JX, Bogue J, Yang J, Corbino K, et al. Comparative genomics reveals 104 candidate structured RNAs from bacteria, archaea, and their metagenomes. Genome Biol. 2010; 11:R31. [PubMed: 20230605]

127. Wickiser JK, Cheah MT, Breaker RR, Crothers DM. The kinetics of ligand binding by an adenine-sensing riboswitch. Biochemistry. 2005; 44:13404–13414. [PubMed: 16201765]

128. Wickiser JK, Winkler WC, Breaker RR, Crothers DM. The speed of RNA transcription and metabolite binding kinetics operate an FMN riboswitch. Mol. Cell. 2005; 18:49–60. [PubMed: 15808508]

129. Wilson RC, Smith AM, Fuchs RT, Kleckner IR, Henkin TM, et al. Tuning riboswitch regulation through conformational selection. J. Mol. Biol. 2011; 405:926–938. [PubMed: 21075119]

130. Winkler W, Nahvi A, Breaker RR. Thiamine derivatives bind messenger RNAs directly to regulate bacterial gene expression. Nature. 2002; 419:952–956. [PubMed: 12410317]

131. Winkler WC, Breaker RR. Regulation of bacterial gene expression by riboswitches. Annu. Rev. Microbiol. 2005; 59:487–517. [PubMed: 16153177]

132. Winkler WC, Cohen-Chalamish S, Breaker RR. An mRNA structure that controls gene expression by binding FMN. Proc. Natl. Acad. Sci. USA. 2002; 99:15908–15913. [PubMed: 12456892]

133. Winkler WC, Nahvi A, Roth A, Collins JA, Breaker RR. Control of gene expression by a natural metabolite-responsive ribozyme. Nature. 2004; 428:281–286. [PubMed: 15029187]

134. Winkler WC, Nahvi A, Sudarsan N, Barrick JE, Breaker RR. An mRNA structure that controls gene expression by binding *S*-adenosylmethionine. Nat. Struct. Biol. 2003; 10:701–707. [PubMed: 12910260]

135. Zhang J, Lau MW, Ferre-D'Amare AR. Ribozymes and riboswitches: modulation of RNA function by small molecules. Biochemistry. 2010; 49:9123–9131. [PubMed: 20931966]

136. Zhao G, Kong W, Weatherspoon-Griffin N, Clark-Curtiss J, Shi Y. Mg^{2+} facilitates leader peptide translation to induce riboswitch-mediated transcription termination. EMBO J. 2011; 30:1485–1496. [PubMed: 21399613]

SUMMARY POINTS

1. Riboswitches demonstrate a large diversity of architectural and metabolite-binding principles that are not always shared within riboswitch families.
2. Similarities and common trends in metabolite binding exist across riboswitch families.
3. Riboswitch folding is directed toward the preformation of the tertiary interactions that facilitates the formation of the ligand-binding-competent conformers.
4. Metabolite recognition and binding by riboswitches appear to be best described by conformational selection and induced-fit models.
5. Riboswitches utilize a diversity of mechanisms for gene expression modulation and exert their function by either thermodynamic or kinetic control.

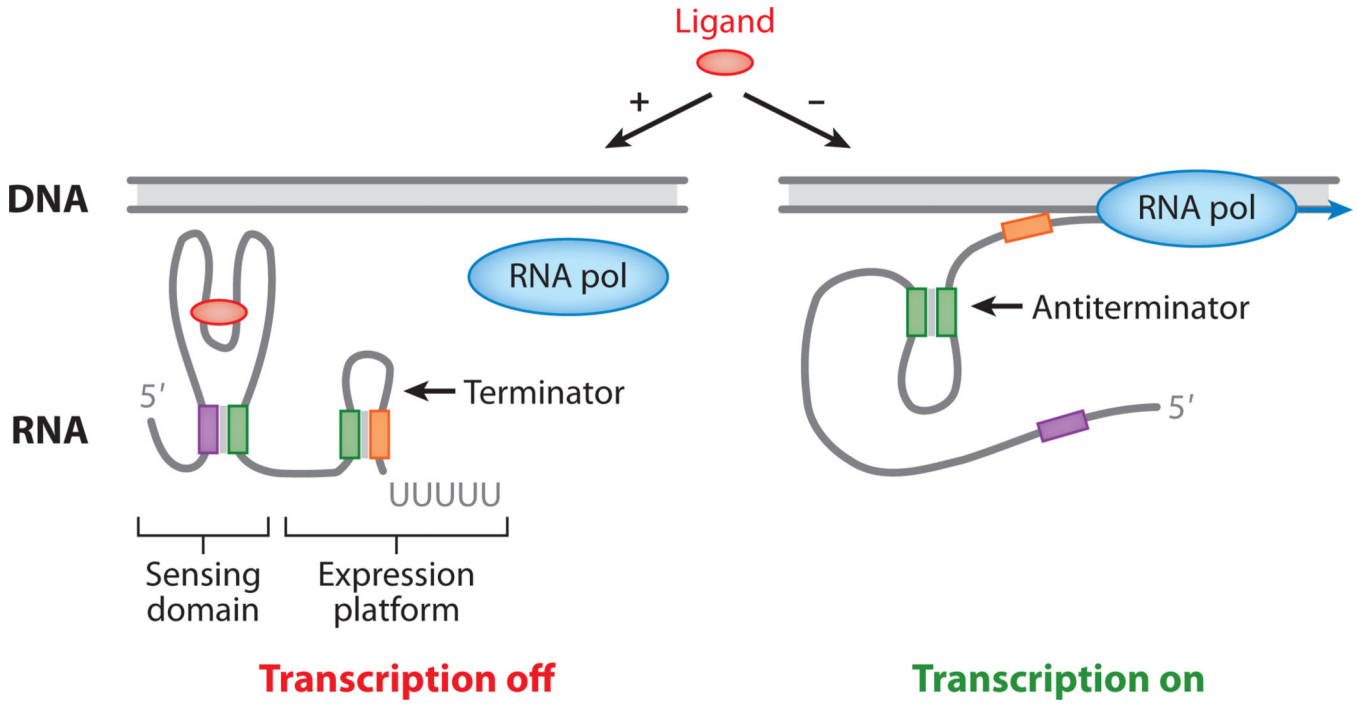

Figure 1.

Transcriptional control mediated by riboswitches. The RNA polymerase (RNA pol) transcribes the metabolite-sensing domain that folds into a stable metabolite-bound RNA conformation in the presence of the cognate metabolite (*left*). This conformation facilitates the formation of the transcription-terminating hairpin in the expression platform and prevents the folding of the alternative antiterminator hairpin, which is formed in the absence of the ligand (*right*). The two RNA conformations cause opposing effects on transcription elongation, prematurely terminating the transcription or allowing the transcription to proceed through the entire gene. Complementary regions of mRNA are shown by colored boxes.

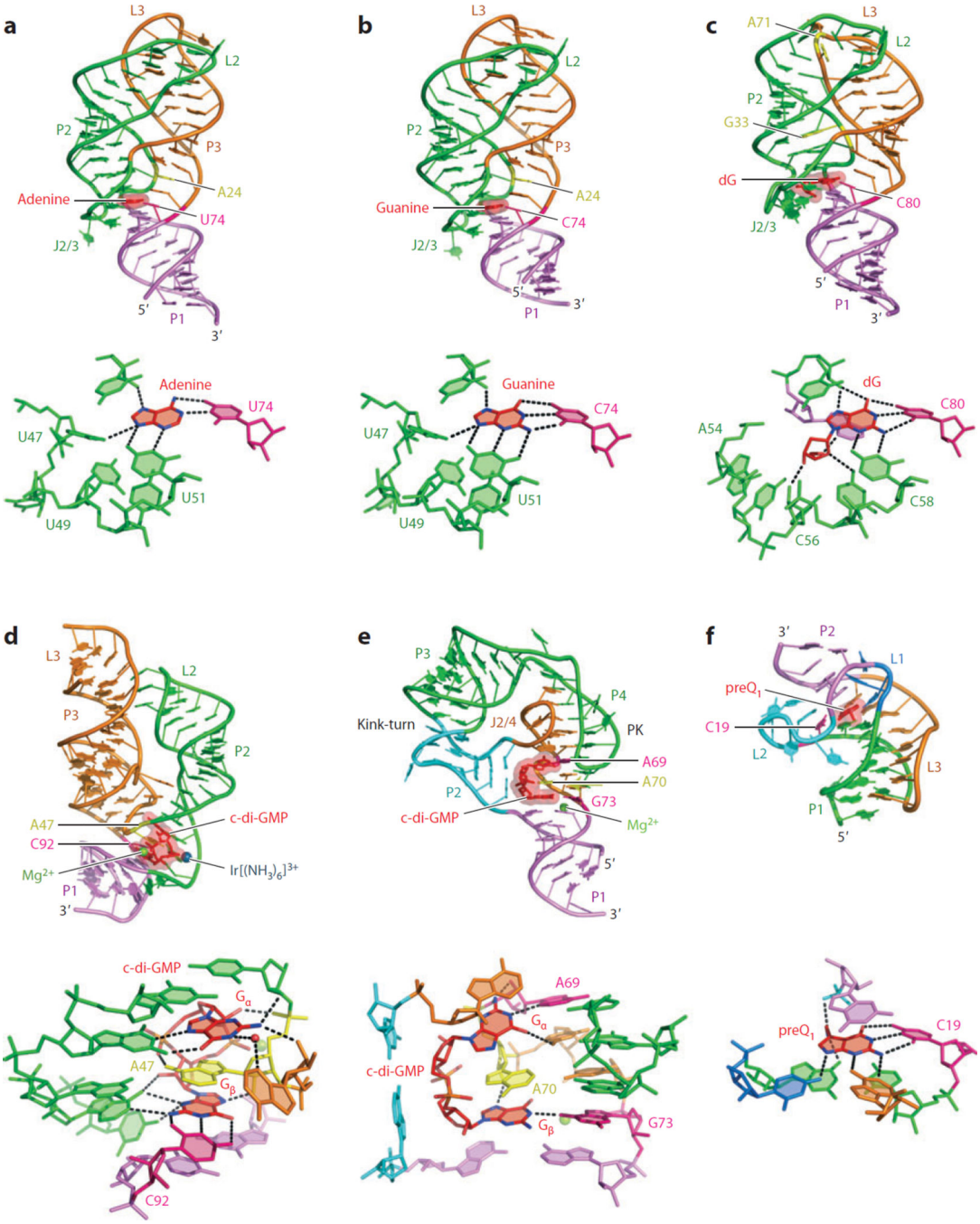

Figure 2.

Three-dimensional structures of metabolite-sensing domains of purine-related riboswitches (*a–f*, *top panels*) and their metabolite-binding pockets (*a–f*, *bottom panels*). The RNA backbone is shown in a ribbon representation. Bound ligands are shown in red sticks and semitransparent surface (*top*). Putative hydrogen bonds between bound metabolites and RNA are shown with dashed lines (*bottom*). Pink nucleotides use their Watson-Crick edge to recognize bound ligands. (*a*) Adenine riboswitch (PDB ID code: 1Y26). The labeled nucleotide highlighted in yellow switches its position from the P3 helix in the adenine and

guanine riboswitches to the P2 helix in the dG riboswitch structure. (*b*) Guanine riboswitch (PDB ID code: 1Y27). (*c*) dG riboswitch (PDB ID code: 3SKI). (*d*) c-di-GMP-I riboswitch (PDB ID code: 3IRW). Nucleotide in yellow is sandwiched between purine bases (G_α and G_β) of the ligand. (*e*) c-di-GMP-II riboswitch (PDB ID code: 3Q3Z). (*f*) $preQ_1$-I riboswitch (PDB ID codes: 2KFC and 3FU2). Abbreviations: c-di-GMP, cyclic di-guanosine monophosphate; dG, 2′-deoxyguanosine; PK, pseudoknot; $preQ_1$, $prequenosine_1$.

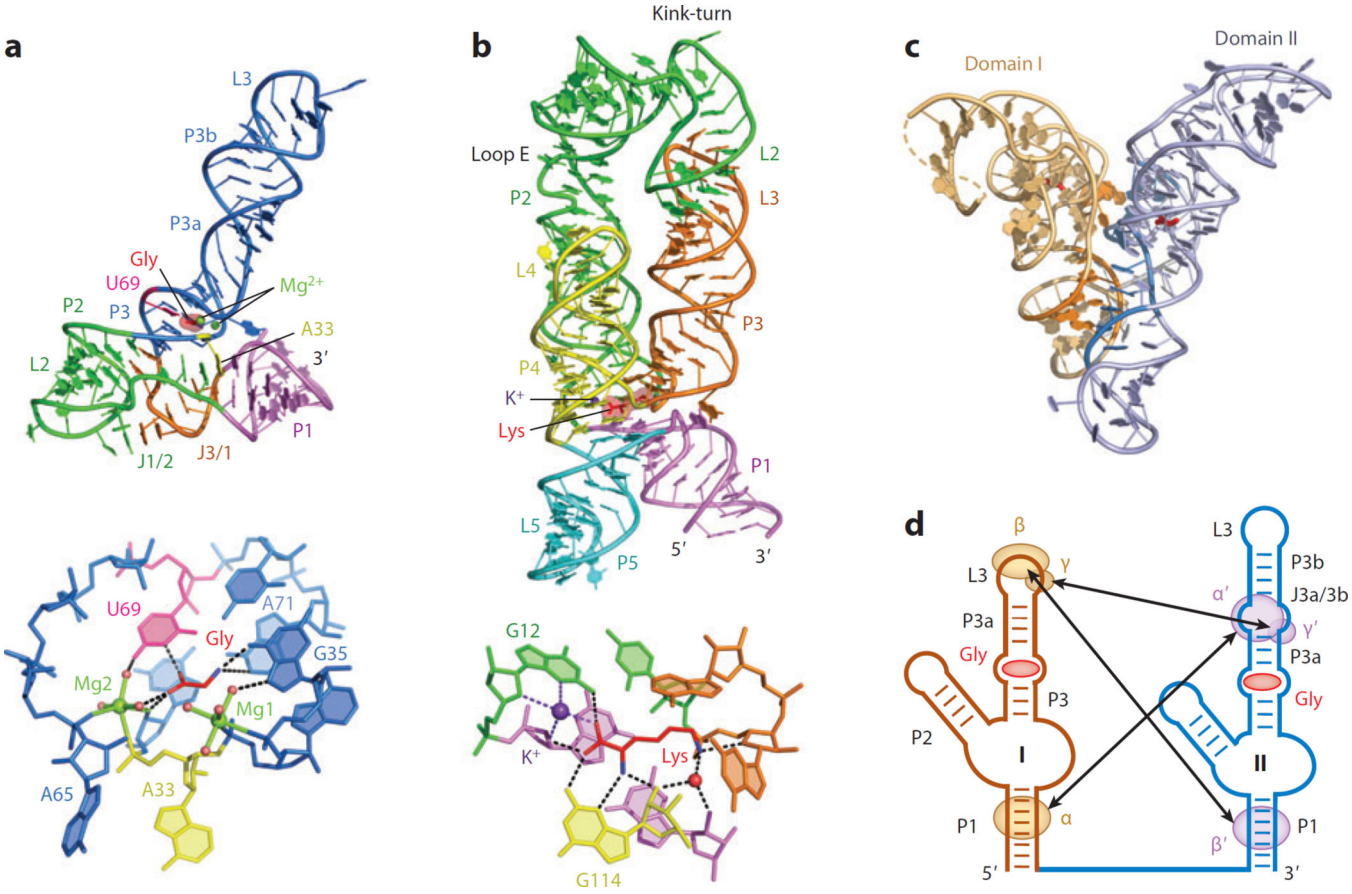

Figure 3.

(*a*,*b*, *top panels*) Structures of metabolite-sensing domains of amino-acid-specific riboswitches, (*a*,*b*, *bottom panels*) details of amino acid recognition, and (*c*,*d*) structural basis of the cooperative control. Water molecules are shown as red spheres. (*a*) Sensing domain II of the *Vibrio cholerae* glycine riboswitch (PDB ID code: 3OWI). Pink nucleotide specifically recognizes glycine. Nucleotide highlighted in yellow is extruded from the ligand-binding pocket and intercalated into the junction. Mg^{2+} coordination bonds are depicted as green sticks. (*b*) Lysine riboswitch (PDB ID code: 3DIL). (*c*) Tandem sensing domains of the cooperative *Fusobacterium nucleatum* glycine riboswitch (PDB ID code: 3P49). Sensing domains I and II are in light orange and light blue, respectively. Residues involved in tertiary interdomain interactions are highlighted in brighter colors. (*d*) Secondary structure schematics of the crystallized *F. nucleatum* glycine riboswitch. Tertiary contact regions are shaded and contacts are indicated with double arrows.

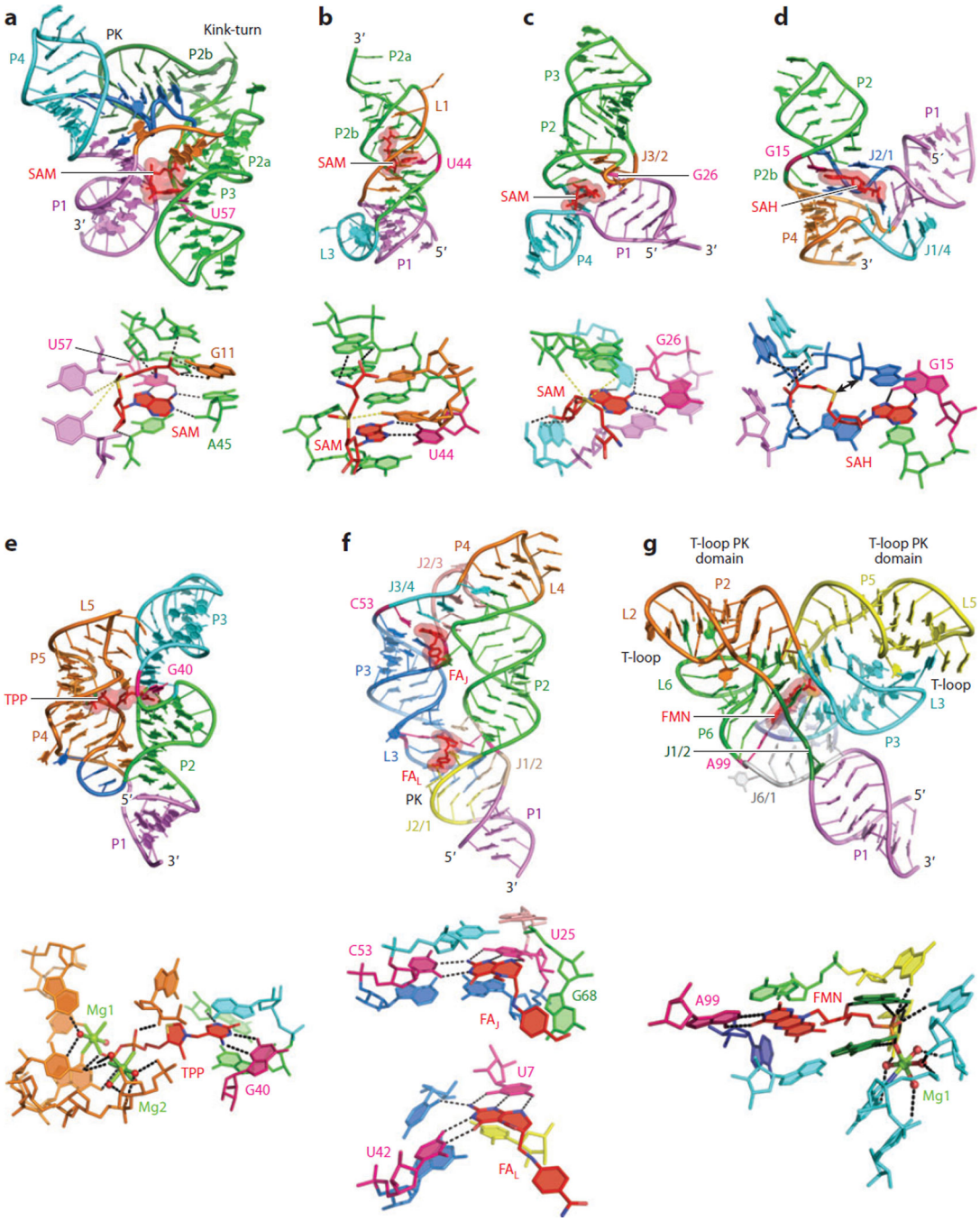

Figure 4.

Structures of metabolite-sensing domains of coenzyme-specific riboswitches (*a–g*, *top panels*) and zoomed-in views of the ligand-binding pockets (*a–g*, *bottom panels*). Pink nucleotides provide base-specific recognition of the ligands. (*a*) SAM-I riboswitch (PDB ID code: 2GIS). Electrostatic interactions are shown with dashed yellow line. (*b*) SAM-II riboswitch (PDB ID code: 2QWY). (*c*) SAM-III riboswitch (PDB ID code: 3E5C). (*d*) SAH riboswitch (PDB ID code: 3NPQ). The double-headed arrow in the bottom panel shows a short distance between the ligand sulfur atom and RNA. (*e*) TPP riboswitch (PDB ID code:

2GDI). Dashed lines show hydrogen bonds between TPP, Mg^{2+} cations, and RNA. (*f*) THF riboswitch bound to two molecules of folinic acid (FA_J and FA_L) (PDB ID code: 3SUH). (*g*) FMN riboswitch (PDB ID code: 3F2Q). Abbreviations: SAM, *S*-adenosylmethionine; SAH, *S*-adenosylhomocysteine; TPP, thiamine pyrophosphate; THF, tetrahydrofolate; FMN, flavin mononucleotide; PK, pseudoknot.

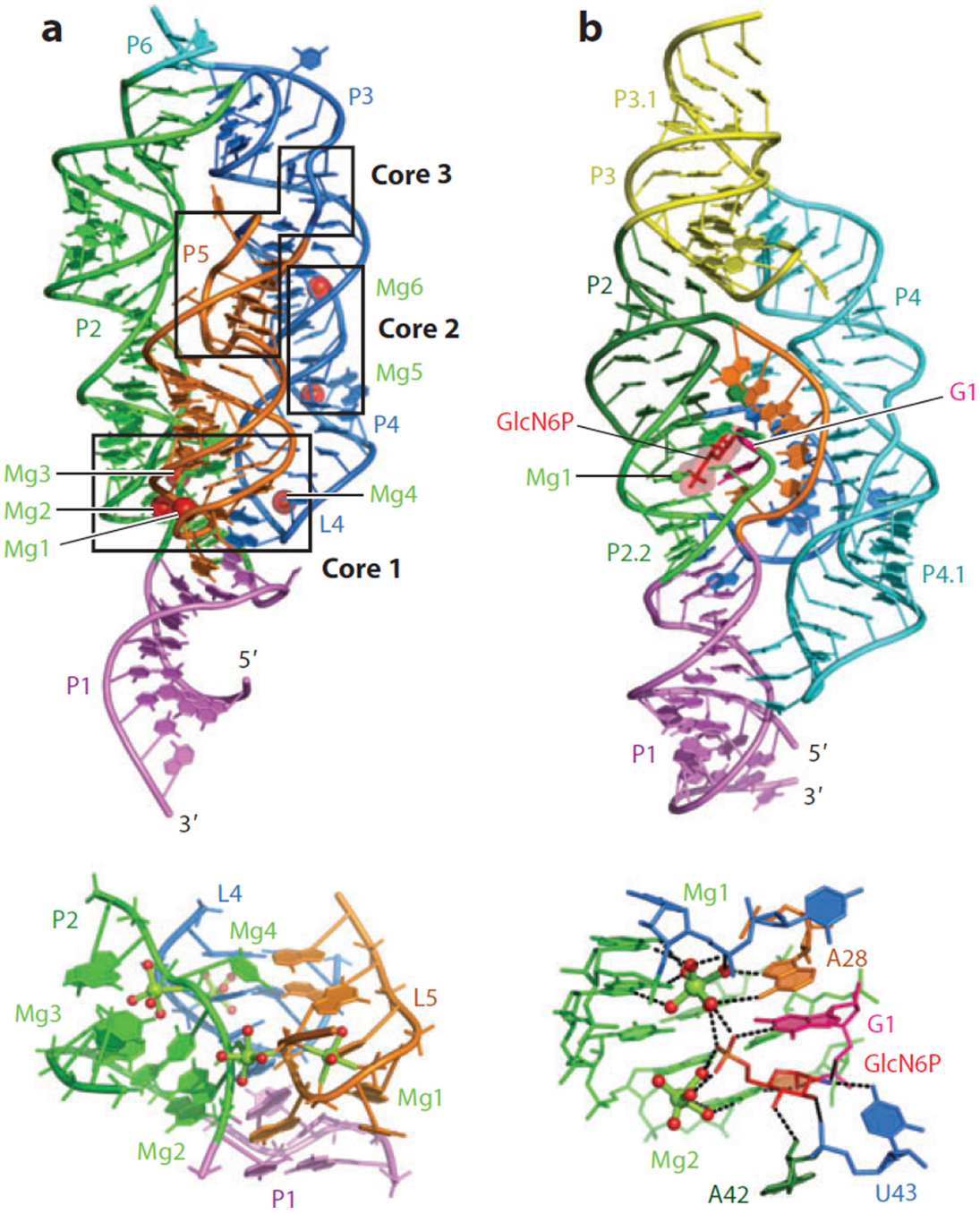

Figure 5.

Structures of complex sensing domains. (*a*, *top panel*) Mg^{2+} sensor (PDB ID code: 2QBZ). Red/green spheres depict crystallographically identified Mg^{2+} cations. Squares show RNA regions where Mg^{2+} cations are clustered. Zoomed-in view of core 1 region is depicted in the bottom panel. (*b*, *top panel*) *glmS* riboswitch/ribozyme (PDB ID code: 2HOZ and 2NZ4). GlcN6P-binding pocket is shown in the bottom panel. Pink color highlights the nucleotide of the cleavage site. Abbreviations: GlcN6P, glucosamine-6-phosphate.

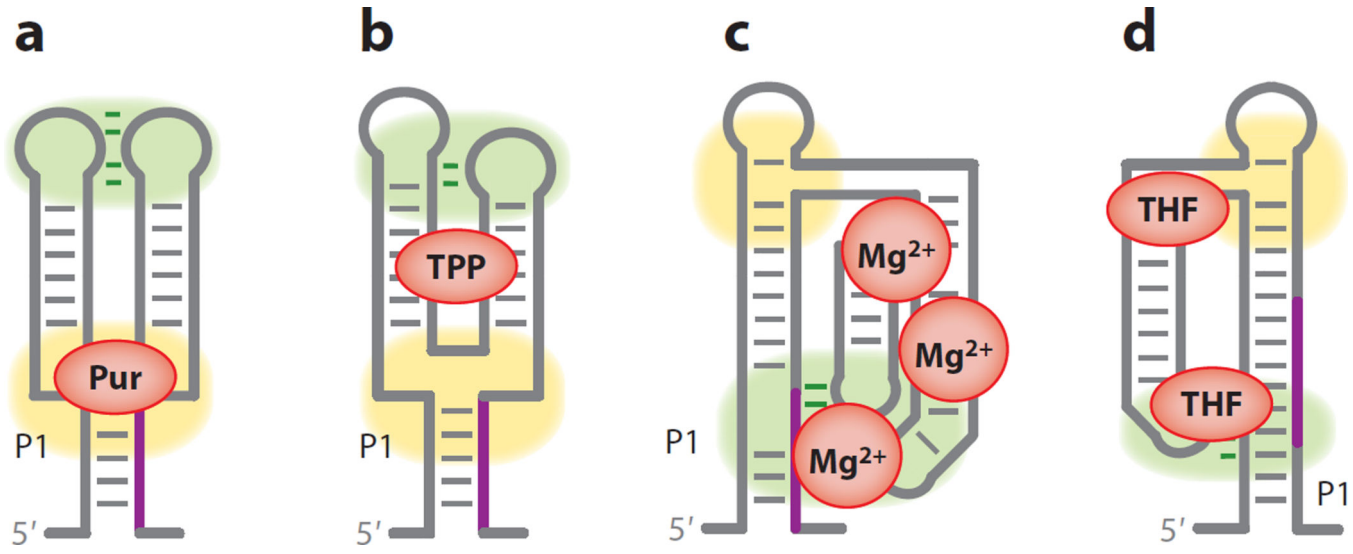

Figure 6.

Schematics of junctional architectures adopted by riboswitches. Yellow and green shadings indicate junctions and regions of long-distance tertiary contacts, respectively. Green lines depict tertiary interactions. Bound ligands are shown with red ovals. Switching sequences are in purple. (*a*) Adenine and (*b*) TPP riboswitches belong to folds with a regular relative position of the junction and the tertiary contact region. (*c*) Mg^{2+} and (*d*) THF riboswitches are characterized by an inverted junctional architecture. Abbreviations: TPP, thiamine pyrophosphate; THF, tetrahydrofolate.

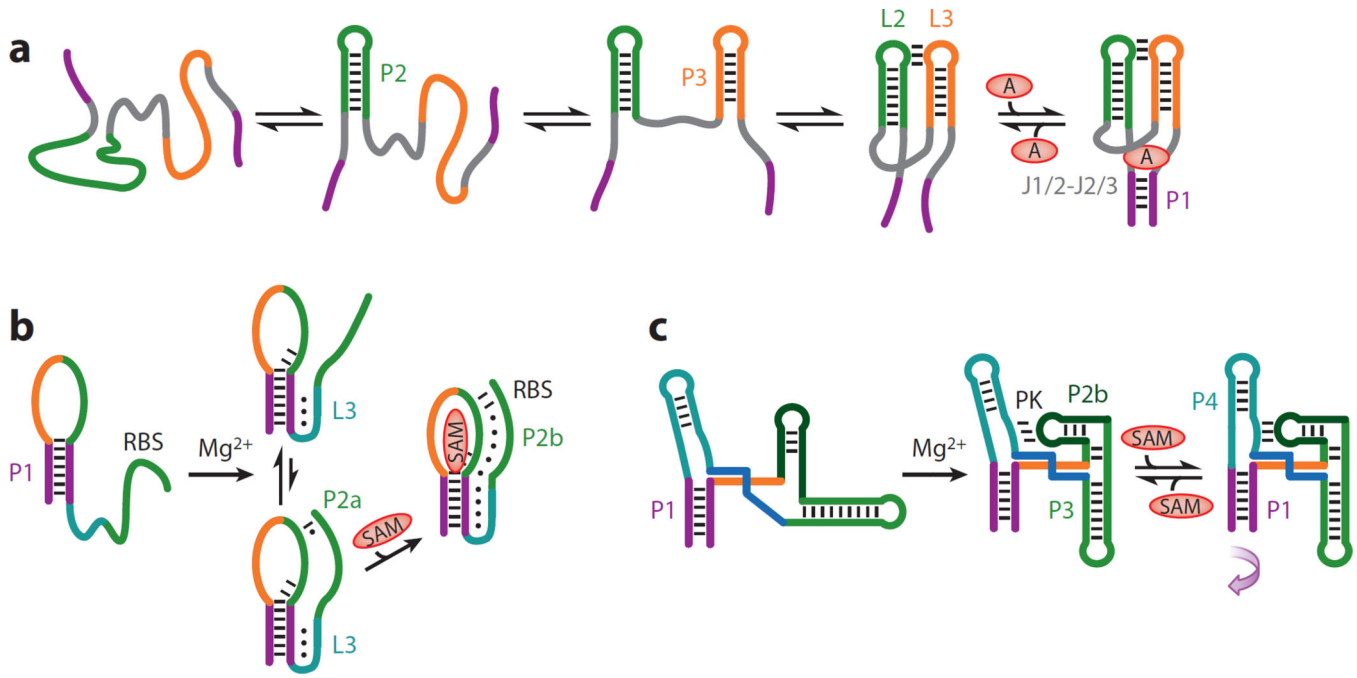

Figure 7.

Global pathways of riboswitch folding. (*a*) Simplified schematics of the *Bacillus subtilis pbuE* adenine riboswitch folding from force spectroscopy experiments (32). Sequential folding of the riboswitch involves the formation of hairpins P2 and P3, followed by the tertiary L2–L3 interactions, docking of adenine to the preorganized junctional core, and stabilization of the regulatory helix P1. (*b*) Conformational capture model of the SAM-II riboswitch folding (35). Mg^{2+} cations stabilize the P1/L3 segment, preorganize the ligand-binding pocket (*top middle panel*), and facilitate the formation of the transient ligand-binding competent pseudoknot-like fold (*bottom middle panel*). SAM selects this transient conformer and induces adaptive rearrangements, resulting in the initial formation of helix P2a and subsequent formation of P2b, together with sequestration of RBS. (*c*) Folding model of the SAM-I riboswitch (38). Mg^{2+} binding preorganizes the ligand-binding conformer by formation of the pseudoknot and the P2/P3 stacking interactions, which position P1 and P3 in close proximity. SAM binding stabilizes stacking between P4 and P1 and rotates helix P1 (*curved arrow*). Abbreviations: RBS, ribosome-binding site; SAM, *S*-adenosylmethionine.

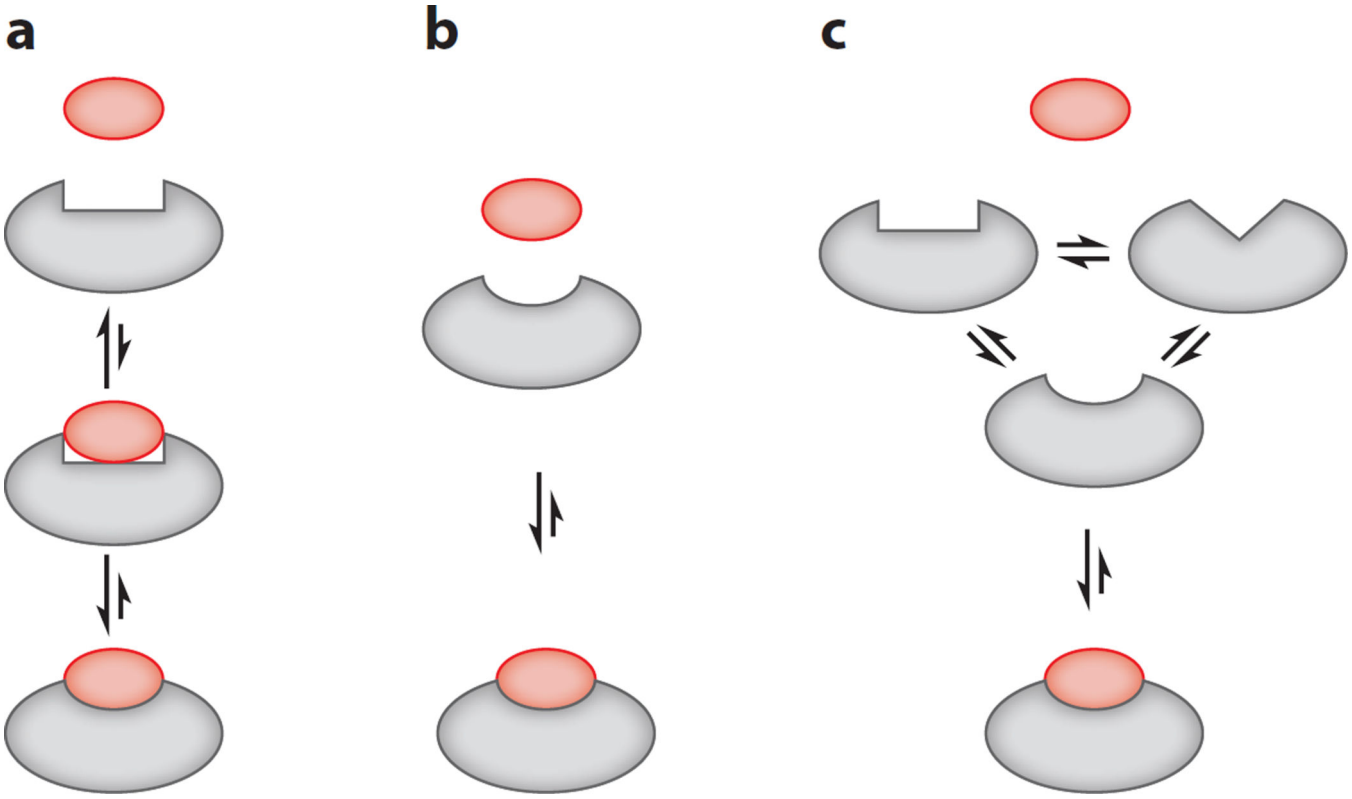

Figure 8.

Models of molecular recognition. (*a*) Induced fit model. Initial contacts between ligand and receptor induce adjustments in the receptor to achieve fully bound riboswitch conformation. (*b*) Lock-and-key model. Ligand fits into the ligand-binding pocket without conformational changes. (*c*) Conformational selection model (9). Binding-competent conformation preexists with other conformations of the sensor and is selected by a cognate ligand to form a ligand-bound complex.

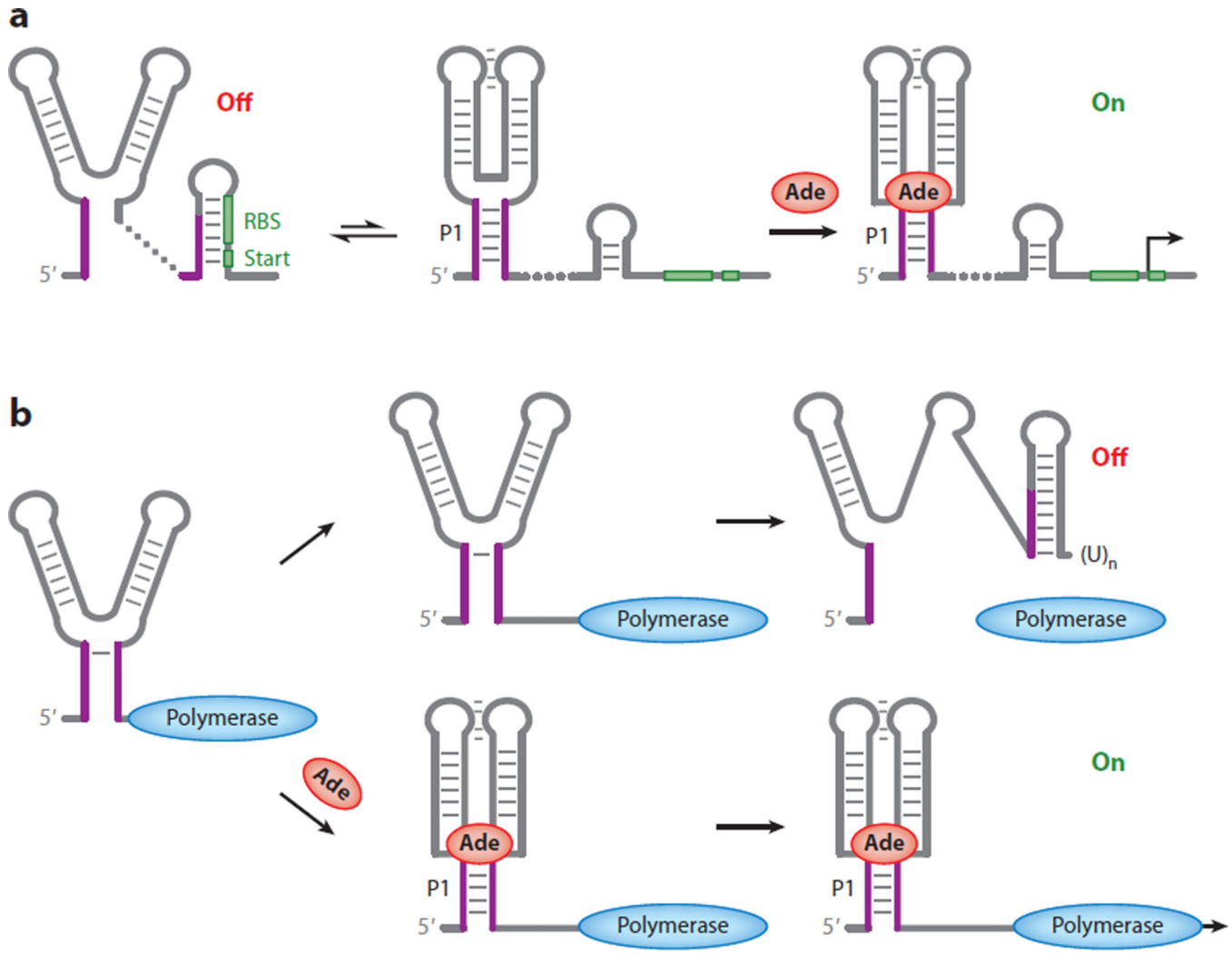

Figure 9.

Regulatory scenarios for adenine riboswitches. (*a*) Thermodynamically driven translation activation by the *Vibrio vulnificus add* riboswitch (36, 59, 92). The equilibrium between translation-repressive (off state) and ligand-binding-competent conformations is shifted by adenine binding toward the ligand-bound conformation that releases RBS and start codon for ribosome binding (on state). (*b*) Kinetically driven transcription activation by the *Bacillus subtilis pbuE* riboswitch (36, 59, 127). After transcription of the sensor is completed, transcription can proceed up to the transcription terminator in the absence of adenine (off state) or through the entire gene if adenine binds and stabilizes the metabolite-bound form that precludes the formation of the terminator (on state). Abbreviations: RBS, ribosome-binding site; Ade, adenine.